Renormalization-group calculations with $k_\parallel$-dependent couplings in a ladder

G. Abramovici, J. C. Nickel, and M. Héritier
Laboratoire de Physique des Solides, associé, au C.N.R.S., Université de Paris Sud, Centre d'Orsay, 91405 Orsay, France
(Received 28 February 2005; published 14 July 2005)

We calculate the phase diagram of a ladder system, with a Hubbard interaction and an interchain coupling $t_\perp$. We use a renormalization-group method, in a one loop expansion, introducing an original method to include $k_\parallel$ dependence of couplings. We also classify the order parameters corresponding to ladder instabilities. We obtain different results, depending on whether we include $k_\parallel$ dependence or not. When we do so, we observe a region with large antiferromagnetic fluctuations, in the vicinity of small $t_\perp$, followed by a superconducting region with a simultaneous divergence of the spin density waves channel. We also investigate the effect of a nonlocal backward interchain scattering: we observe, on one hand, the suppression of singlet superconductivity and of spin density waves, and, on the other hand, the increase of charge density waves and, for some values of $t_\perp$, of triplet superconductivity. Our results eventually show that $k_\parallel$ is an influential variable in the renormalization-group flow, for this kind of system.

DOI: 10.1103/PhysRevB.72.045120 PACS number(s): 71.10.Li, 71.10.Pm, 71.10.Fd, 74.20.−z

I. INTRODUCTION

The physics of ladder systems remains a source of considerable interest. In the past decades, many conductors were found, with anisotropic two-leg electronic structure, such as $SrCu_2O_3$ (Ref. 1) or $Sr_{14-x}Ca_xCu_{24}O_{41}$ (Ref. 2) compounds. The structure of $La_2Cu_2O_5$ (Ref. 3) can also be analyzed as weakly coupled ladders, and is therefore very similar. The phase diagram of these compounds is very rich; it is now well established that these systems behave like Luttinger liquids at high temperature, while they can behave like Fermi liquids when T decreases; they exhibit superconducting (SC) phases of type II, which can also be mixed with antiferromagnetic fluctuations. In some case, the SC phase is found to be spin-gapped, while spinless phases are also reported.[4]

From a theoretical point of view, the ladder (or two-coupled chain) model is the simplest quasi-one-dimensional one. Although all its properties are not entirely elucidated, it has been used by many authors as a toy model, to build and explore new approaches (two-leaf dispersion models calculated by a Kadanoff-Wilson renormalization method[5] or by a bosonization method;[6] transition between commensurate and incommensurate filling,[7] in particular close to the half-filing case;[8,9] dimensional transition,[10] etc.). These systems have been intensively used to investigate nonconventional SC process (with singlet[11–13] or triplet[14] pairing).

This paper is devoted to the study of a ladder model, with a Hubbard interaction (U is the Hubbard constant) and an interband coupling ($t_\perp$ is the interaction factor), at zero temperature. We investigate the phase diagram in the range of parameter $0 \leqslant U \leqslant 8\pi t_\parallel \eta$ and suppose that the electronic filling η is incommensurate. Although there is yet no evidence for the existence of compounds lying in this range of parameter, we have hopes that some of these will indeed be found and confirm the theoretical predictions that we present here.

The phase diagram of this system has been partially studied by several authors. In particular, Fabrizio has used a renormalization group (RG) method, in a two-loop expansion from the Fermi liquid solution.[12] He includes interband backward scattering g_b, and, within the range of parameter that we have investigated, finds a SC phase, named "phase I," which he clearly points out not to be singlet s, although he did not elucidate the symmetry of the condensate. In his calculations, the RG flow of susceptibilities shows several divergences: the spin density wave (SDW) channel coexists with the superconducting one. This author did alternatively cut the flow before the divergences and bozonize the effective Hamiltonian; then, SDW modes disappear and are replaced by charge density wave (CDW) instabilities.

These results are more or less compatible with that of other methods, using a one-loop expansion,[15,16] or bozonizing the Hamiltonian of the bare system[17–20] (see also Ref. 13), or using quantum Monte Carlo method.[21] These authors generally find a singlet superconducting condensate of symmetry d, which coexists with SDW or CDW instabilities. This complicated phase has also been related to the RVB phase.[22] One of the central questions is whether the SC modes are spin-gapped or not, and receives various and even contradictory answers. Using a two-loop expansion, Kishine[23] observes a spin gap, which is suppressed when $t_\perp \to 0$. This is also the result found with a density matrix RG method by Park.[24]

We give a new insight into these questions, using a RG method, in a perturbative expansion in U. This kind of method has been used in many recent and very complete works.[25–27] Here, we calculate RG equations with one loop diagrams, including g_b couplings, as in Ref. 12, as well as all parallel momentum dependence.

Let us emphasize that, although we begin from the Fermi liquid solution, we find a phase with only SDW fluctuations, for small enough interband interaction $t_\perp \leqslant t_{\perp c}(U)$, contrary to all previous results obtained by RG methods, which always indicate SC instabilities as soon as $t_\perp \neq 0$ (see for instance Lin *et al.*[15]). However, this phase is different from the one-dimension limit. This is a very remarkable result, since $k_\parallel$ is known to be an irrelevant variable of the RG flow.[28] However, we will prove in this paper that it is indeed influential in the very case of a ladder.

When $t_\perp$ is increased, we observe a transition at $t_{\perp c}$ to a superconducting phase, where singlet SC instabilities of

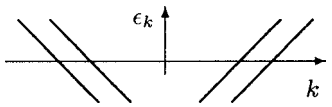

FIG. 1. The 2-band dispersion in ∥ direction.

symmetry d coexist with SDW ones. This phase is found by many authors (see Refs. 12, 15, and 16 and other articles already quoted).

Recently, Bourbonnais *et al.*[29,30] have examined the effect of interchain Coulomb interactions for an infinite number of coupled chains, using RG method. Interchain backward scattering was found to enhance CDW fluctuations and favor triplet instead of singlet SC. Here we investigated the effect of a Coulomb interchain backward interaction C_{back} for the ladder problem. We find that this interaction favors triplet SC instabilities instead of singlet ones and CDW instabilities instead of SDW ones in a ladder system too. Indeed, both the singlet SC and SDW instabilities (if any) are suppressed when C_{back} is increased, and we observe triplet SC as well as CDW instabilities. The triplet SC existence region is however very narrow and lies inside the region $t_\perp \geqslant t_{\perp c}(U)$. For large values of C_{back} ($C_{\text{back}} \sim U$), CDW is always dominant; this is consistent with what Lin *et al.* find.[15]

On the contrary, when a Coulombian interchain forward interaction C_{for} is added, all SC instabilities are depressed, and we only observe SDW and CDW fluctuations.

We also present a detailed classification of the pair operators in a ladder, which are connected to the order parameters. It proves a very powerful tool in these sophisticated RG methods.

So, we will first give a short description of the model (in Sec. II), then present the classification of the pair operators (in Sec. III, the symmetries are explained in Appendix C), then we explain the RG formulation and techniques that are used here (in Sec. IV). Results concerning only initially local interactions are presented in Sec. V, while those concerning the influence of additional interchain interactions are given in Sec. VI. In Sec. VII we conclude.

II. MODEL

The Hubbard model of a ladder has been studied in various articles. We give here a brief presentation of this model (see Refs. 12 or 31 with similar notations).

A. Kinetic Hamiltonian

1. The model in a 1D representation

The dispersion curve separates into two bands (0 and π), so the Fermi surface splits into four points ($-k_{f0}$, $-k_{f\pi}$, $k_{f\pi}$, k_{f0} in the ∥ direction, + corresponds to right moving particles and − to left moving ones). The bands are linearized around the Fermi vectors[32] with a single Fermi velocity v_f (cf. Fig. 1). We write R the right moving particles and L the left moving ones. Then, the kinetic Hamiltonian writes

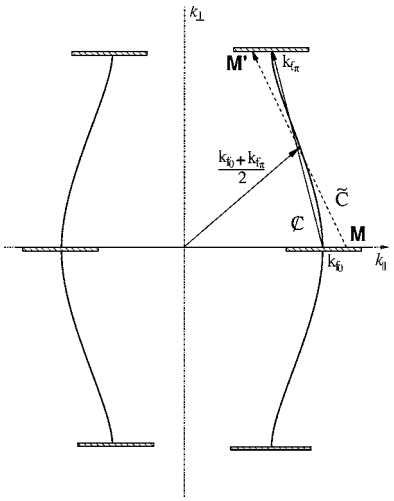

FIG. 2. Two-dimensional representation of the states. The physical space, for a ladder, is restricted to the hatched bands at $k_\perp = 0$ and $k_\perp = \pm \pi/b$. The curves correspond to the Fermi surface of a 2D system, with an infinite number of chains. The four Fermi points, in the ladder system, are the intersections of these curves with the physical bands. The symmetry $\tilde{C}$ that maps point M onto M' is the point symmetry around the affine point, corresponding to $(k_{f0} + k_{f\pi})/2$. The symmetry $\mathcal{C}$ is the translation by the vector $k_{f0} - k_{f\pi}$, which is also represented by a plain arrow.

$$H_{\text{cin}} = \sum_\sigma v_f \Bigg(\sum_K (K - k_{f0}) R^\dagger_{0\sigma}(K) R_{0\sigma}(K) + \sum_K (K - k_{f\pi}) R^\dagger_{\pi\sigma}(K) R_{\pi\sigma}(K) + \sum_K (K + k_{f0}) L^\dagger_{0\sigma}(K) L_{0\sigma}(K) + \sum_K (K + k_{f\pi}) L^\dagger_{\pi\sigma}(K) L_{\pi\sigma}(K) \Bigg). \tag{1}$$

We define the Fermi surface gap $\Delta k_f = k_{f0} - k_{f\pi}$. One then gets $\Delta k_f = 2t_\perp / v_f$. The discretization step in ∥ direction is a, and the reciprocal vector in this direction is defined modulo $2\pi/a$. The distance between the chains in ⊥ direction is b.

In order to give a clear representation of all instability processes that will be discussed afterwards, it is worth showing how this model can be embedded in a 2D representation, which we present now.

2. The model in a 2D representation

The general 2D dispersion law writes

$$\epsilon(\mathbf{k}) = -2t_\parallel \cos(k_\parallel a) - 2t_\perp \cos(k_\perp b)$$

as represented in Fig. 2; if one writes approximately $k_f \approx k_{f0} \approx k_{f\pi}$, one gets $v_f \approx 2at_\parallel \sin(k_f a)$. In real space, $y_\parallel$ corresponds to the axis along the chains, and $y_\perp$ takes only two values, $y_\perp = \pm 1$, corresponding to which chain one refers to. The ∥ axis is then discretized, $y_\parallel = 1 \ldots N$, where $4N$ is the total number of states. The Fourier transformation from real space functions to reciprocal space ones is detailed in Appendix D.

From $y_\perp=\pm 1$, one gets $k_\perp=0$ or $\pm\pi/b$ ($k_\perp=\pi/b$ and $k_\perp=-\pi/b$ are identified). Therefore, the physical states are limited to the four horizontal bands, shown in Fig. 2, which are centered on each of the four Fermi points. The two bands centered on $(\pm k_{f0},0)$ are the left and right bands 0 (L_0 or R_0), the two bands centered on $(\pm k_{f\pi},\pi/b)$ are the left and right bands π (L_π or R_π).

B. Interaction Hamiltonian

The most general interaction Hamiltonian can be written, with $L_{\mathbf{k}\sigma}=L_{0\sigma}(K)$ for $\mathbf{k}=(K,0)$, $L_{\mathbf{k}\sigma}=L_{\pi\sigma}(K)$ for $\mathbf{k}=(K,\pi)$ and idem for R,

$$H_{\text{int}}=\frac{1}{N}\sum_{\substack{\mathbf{k}_1,\mathbf{k}_2,\mathbf{k}_1',\mathbf{k}_2'\\ \mathbf{k}_1+\mathbf{k}_2=\mathbf{k}_1'+\mathbf{k}_2'}}\sum_{\sigma_1,\sigma_2}\mathcal{G}_1(\mathbf{k}_1,\mathbf{k}_2,\mathbf{k}_2',\mathbf{k}_1')\times R^\dagger_{\mathbf{k}_1'\sigma_1}L^\dagger_{\mathbf{k}_2'\sigma_2}R_{\mathbf{k}_1\sigma_2}L_{\mathbf{k}_2\sigma_1}+\mathcal{G}_2(\mathbf{k}_1,\mathbf{k}_2,\mathbf{k}_2',\mathbf{k}_1')\times R^\dagger_{\mathbf{k}_1'\sigma_1}L^\dagger_{\mathbf{k}_2'\sigma_2}L_{\mathbf{k}_2\sigma_2}R_{\mathbf{k}_1\sigma_1},\tag{2}$$

where $\mathcal{G}_\alpha$ is the two-particle coupling, and we have used the g-ology representation. We do not include umklapp interactions $\mathcal{G}_3$ ($LLRR$ or $RRLL$) nor $\mathcal{G}_4$ terms ($LLLL$ or $RRRR$). We will alternatively use the singlet-triplet representation, where α takes values $\alpha=s,t$, or the Charge-Spin representation, where $\alpha=C,S$. If not necessary, we will omit the spin dependence α. Equations (A1) and (A2) give, in Appendix A 1, the usual relations between these different representations.

We distinguish, following Fabrizio,[12] g_0, which corresponds to $R_0^\dagger L_0^\dagger L_0 R_0$ process, $g_\pi(\leftrightarrow R_\pi^\dagger L_\pi^\dagger L_\pi R_\pi)$, $g_{f0}(\leftrightarrow R_0^\dagger L_\pi^\dagger L_\pi R_0)$, $g_{f\pi}(\leftrightarrow R_\pi^\dagger L_0^\dagger L_0 R_\pi)$, $g_{t0}(\leftrightarrow R_0^\dagger L_0^\dagger L_\pi R_\pi)$, $g_{t\pi}(\leftrightarrow R_\pi^\dagger L_\pi^\dagger L_0 R_0)$, $g_{b0}(\leftrightarrow R_0^\dagger L_\pi^\dagger L_0 R_\pi)$ and $g_{b\pi}(\leftrightarrow R_\pi^\dagger L_0^\dagger L_\pi R_0)$. The definitions of these couplings, including the $k_\parallel$ dependence are detailed in Appendix A 1 and Fig. 18; from symmetry considerations, one only needs g_0, g_π, g_{f0}, g_{t0} and g_{b0}; in fact, we will see that even g_π can be deduced from g_0 in the very case of a ladder, so that we only deal with four couplings.

Bare couplings. Of course, in the initial Hubbard model, the two-particle couplings do not depend on the momenta. We will define $\tilde{U}=Ua/(\pi v_f)$ and $\tilde{g}=ga/(\pi v_f)$, to get rid of the physical dimensions. Then, the bare couplings values are simply $\tilde{g}_i=\tilde{U}$.

Additional Coulombian interchain interactions. The above Hamiltonian H_{int} corresponds to local interactions. We have also studied the effect of additional Coulombian interchain interactions.

In order to implement a backward interchain interaction, we need to modulate the bare parameters, which simply writes, in this case, $\tilde{g}_{01}=\tilde{U}+\tilde{C}_{\text{back}}$, $\tilde{g}_{f01}=\tilde{U}-\tilde{C}_{\text{back}}$, $\tilde{g}_{t01}=\tilde{U}-\tilde{C}_{\text{back}}$ and $\tilde{g}_{b01}=\tilde{U}+\tilde{C}_{\text{back}}$, where $\tilde{C}_{\text{back}}=C_{\text{back}}a/(\pi v_f)$ is the corresponding interaction factor.

When we include instead a forward interchain interaction, of parameter $\tilde{C}_{\text{for}}=C_{\text{for}}a/(\pi v_f)$, the modulation of the bare parameters writes $\tilde{g}_{02}=\tilde{U}+\tilde{C}_{\text{for}}$, $\tilde{g}_{f02}=\tilde{U}+\tilde{C}_{\text{for}}$, $\tilde{g}_{t02}=\tilde{U}-\tilde{C}_{\text{for}}$ and $\tilde{g}_{b02}=\tilde{U}-\tilde{C}_{\text{for}}$.

Eventually, if we include both interactions, we only need to add the two modulations.

C. External excitation fields

We note $\mathcal{Z}$ the three-legged couplings to external excitation fields. We will write $\mathcal{Z}_\alpha^{\text{DW}}$, $(\alpha=C,S)$ for Charge or spin density waves, and $\mathcal{Z}_\alpha^{\text{SC}(\Gamma)}$, $(\alpha=s,t)$ for singlet or triplet superconducting states of symmetry $\Gamma=s,p,d,f,g$. Again, we will omit index α as soon as it is not necessary, and distinguish z_0^{DW}, which corresponds to $L_0^\dagger R_0$ process, $z_\pi^{\text{DW}}(\leftrightarrow L_\pi^\dagger R_\pi)$, $z_+^{\text{DW}}(\leftrightarrow L_\pi^\dagger R_0)$ and $z_-^{\text{DW}}(\leftrightarrow L_0^\dagger R_\pi)$. The first process corresponds to an intraband mapping that relates 0-band states (horizontally in the 2D representation of Fig. 2), idem for the second one with π-band ones, while the last ones are interband mappings (biased in Fig. 2); the same applies to $\mathcal{Z}^{\text{SC}}$, except that the processes now write L_0R_0, $L_\pi R_\pi$, L_0R_π, and $L_\pi R_0$. The definitions of all these couplings are detailed in Appendix A 2 and Fig. 19; from symmetry considerations, one only needs z_0, z_π and z_+; again, in the very case of a ladder, we will see that z_π can also be deduced from z_0, so we only deal with two couplings per instability.

With our specific choice, the initial values of the couplings to external fields are all $z_i=1$.

After this brief presentation of the model, we will now expound the classification of the different instabilities, according to their symmetries, which we will study afterwards.

III. RESPONSE FUNCTIONS

To each external excitation field corresponds a susceptibility, which is the response function of a pair operator. The corresponding order parameter is the mean value of this operator. In order to classify the different instabilities, one just needs to classify the pair operators. Their symmetries are detailed in Appendix C.

We will first begin with SC instabilities.

A. Superconducting instabilities

1. SC Hamiltonian

Let us define the superconducting order parameters $\Delta_\alpha^{(\Gamma)}(\mathbf{X})=\langle O_\alpha^{(\Gamma)}(\mathbf{X})\rangle$, where the electron-electron pair operator writes $O_\alpha^{(\Gamma)}=\Sigma_{\mathbf{X}'\sigma\sigma'}\psi_{\mathbf{X},\sigma}\Gamma(\mathbf{X},\mathbf{X}')\psi_{\mathbf{X}',\sigma'}\tau^\alpha_{\sigma\sigma'}$, with $\tau^s=\mathrm{i}\sigma_y$ for singlet states, $\tau^{tx}=\mathrm{i}\sigma_x\sigma_y=-\sigma_z$, $\tau^{ty}=\mathrm{i}\sigma_y\sigma_y=\mathrm{i}I$ and $\tau^{tz}=\mathrm{i}\sigma_z\sigma_y=\sigma_x$ for triplet states (σ_i are the Pauli matrix, I is the 2×2 identity matrix and i is the imaginary number). $\psi_{\mathbf{X},\sigma}$ is a real space wave function; since electrons occupy discrete positions $\mathbf{X}=(ia,bj/2)$ $(i=1\ldots N,\ j=\pm 1)$, we will rather write $\psi_{ij\sigma}$. The corresponding Hamiltonian writes, in reciprocal space variables,

$$H_{\text{SC}}=\sum_{\substack{\mathbf{P}_1,\mathbf{P}_2\\ \sigma_1,\sigma_2}}\bar{\mathcal{Z}}^{\text{SC}}(\mathbf{P}_1,\mathbf{P}_2,\mathbf{Q})\tau^{(\alpha)}\phi_{\mathbf{Q}}\Psi_{\mathbf{P}_1\sigma_1}\Psi_{\mathbf{P}_2\sigma_2}+\mathcal{Z}^{\text{SC}}(\mathbf{P}_1,\mathbf{P}_2,\mathbf{Q})\bar{\tau}^{(\alpha)}\phi^\dagger_{\mathbf{Q}}\Psi^\dagger_{\mathbf{P}_2\sigma_2}\Psi^\dagger_{\mathbf{P}_1\sigma_1},\tag{3}$$

where $\mathbf{Q}=(Q_\parallel,Q_\perp)=\mathbf{P}_1+\mathbf{P}_2$ is the interaction momentum.

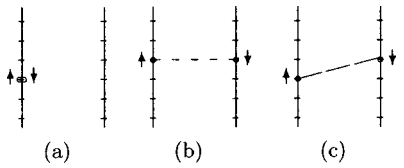

FIG. 3. Real space representation of SC condensate of singlet s symmetry (a), d (b), and g (c).

In order to simplify our expressions in this section, we write $L_{p,\theta,\sigma}=L_{\theta,\sigma}(p-k_{f\theta})$ and $R_{p,\theta,\sigma}=L_{\theta,\sigma}(p+k_{f\theta})$, where $\theta=0,\pi$. Notation $\int_L$ stands for the half band integration $\int_{k_{f0}-\pi/a}^{k_{f0}}$ or $\int_{k_{f\pi}-\pi/a}^{k_{f\pi}}$, in which case we will not need to be precise, since what takes place at the band limit is not physically relevant, in this system.

To each order parameter $\Delta(\mathbf{X})$ corresponds to an infinite number of Fourier componants, depending on the reciprocal space variable $\mathbf{Q}$. We will only keep components $\mathbf{Q}=(0,0)$ and $\mathbf{Q}=(\pm\Delta k_f,\pi/b)$, so that $\epsilon(\mathbf{k})$ and $\epsilon(\mathbf{Q}-\mathbf{k})$ both lie in the physical band, close to the Fermi points. We will write, in short, $O(0)$ and $O(\pi_\pm)$ as the corresponding pair operators.

Let us now classify the different operators, according to their symmetry, by choosing the adequate Γ. The principles of the calculation and some details are given in Appendix D.

2. Singlet s condensates

The local pairing $\Gamma(\mathbf{X},\mathbf{X}')=\delta_{ii'}\delta_{jj'}$ gives singlet condensates of s symmetry. The pair operator reduces to

$$O_s^{(s)}(\mathbf{X})=2\psi_{\mathbf{X}\uparrow}\psi_{\mathbf{X}\downarrow}=2\psi_{ij\uparrow}\psi_{ij\downarrow}.$$

$O(0)$ component corresponds to an intraband pairing, named 0-condensate ($\mathbf{Q}=\mathbf{0}$, corresponding to z_0^{SC}, see Appendix A 2 and writes

$$\begin{aligned}O_s^{(s)}(0)&=2\sum_i \psi_{i,1\uparrow}\psi_{i,1\downarrow}+\psi_{i,-1\uparrow}\psi_{i,-1\downarrow}\\&=\int_L\frac{adp}{2\pi}L_{p,0\uparrow}R_{-p,0\downarrow}+L_{p,\pi\uparrow}R_{-p,\pi\downarrow}+R_{-p,0\uparrow}L_{p,0\downarrow}\\&\quad+R_{-p,\pi\uparrow}L_{p,\pi\downarrow}.\end{aligned}$$

$O(\pi_\pm)$ component corresponds to an interband pairing, named π condensate [$\mathbf{Q}=(\pm\Delta k_f,\pi/b)$, corresponding to z_+^{SC}, see Appendix A 2] and writes

$$\begin{aligned}O_s^{(s)}(\pi_\pm)&=-2\mathrm{i}\sum_i e^{\mp\mathrm{i}\Delta k_f ia}(\psi_{i,1\uparrow}\psi_{i,1\downarrow}-\psi_{i,-1\uparrow}\psi_{i,-1\downarrow})\\&=-\mathrm{i}\int_L\frac{adp}{2\pi}L_{p,0\uparrow}R_{\Delta k_f(1\pm1)-p,\pi\downarrow}+L_{p,\pi\uparrow}R_{\Delta k_f(-1\pm1)-p,0\downarrow}\\&\quad+R_{\Delta k_f(-1\pm1)-p,0\uparrow}L_{p,\pi\downarrow}+R_{\Delta k_f(1\pm1)-p,\pi\uparrow}L_{p,0\downarrow}.\end{aligned}$$

It is however antisymmetric with parity $[PO_s^{(s)}(\pi/b)=-O_s^{(s)}(\pi/b)]$; this comes from the $e^{-\mathrm{i}Q_\perp jb/2}$ factor in the Fourier calculation; see details in Appendix D.

The s condensates are local in real space; see Fig. 3(a).

If Γ is replaced by $\delta_{i,i'\mp m}\delta_{jj'}$, one gets extended s states (in reciprocal space variables, the components are multiplied by $\cos(mPa)$ or some similar factor; see some examples in Appendix D). However, we did not include these in our calculations.

3. Singlet d and g condensates

There are also two singlet condensates of d and g symmetry.

With $\Gamma=\delta_{i,i'}\delta_{j,-j'}$ (interchain pairing, with equal positions on each chain), one gets another pair operator. $O_s(\pi)$ component is zero for singlet condensate, while $O(0)$ component corresponds to an intraband pairing (0 condensate) of d symmetry, and writes

$$\begin{aligned}O_s^{(d)}(0)&=2\sum_i \psi_{i,1\uparrow}\psi_{i,-1\downarrow}+\psi_{i,-1\uparrow}\psi_{i,1\downarrow}\\&=\int_L\frac{adp}{2\pi}L_{p,0\uparrow}R_{-p,0\downarrow}-L_{p,\pi\uparrow}R_{-p,\pi\downarrow}+R_{-p,0\uparrow}L_{p,0\downarrow}\\&\quad-R_{-p,\pi\uparrow}L_{p,\pi\downarrow}.\end{aligned}$$

With $\Gamma=\delta_{i,i'\mp1}\delta_{j,-j'}$, one gets a more complicated pair operator. $O(\pi)$ component corresponds to an interband pairing (π condensate) of g symmetry, and writes

$$\begin{aligned}O_s^{(g)}(\pi_\pm)&=-2\mathrm{i}\sum_i e^{\mp\mathrm{i}\Delta k_f ia}(\psi_{i,1\uparrow}\psi_{i+1,-1\downarrow}-\psi_{i,-1\uparrow}\psi_{i+1,1\downarrow})\\&=-e^{\pm\mathrm{i}(\Delta k_f a/2)}\int_L\frac{adp}{2\pi}\sin\left(a\left(p-k_{f0}\mp\frac{\Delta k_f}{2}\right)\right)\\&\quad\times(L_{p-\Delta k_f,\pi\uparrow}R_{\pm\Delta k_f-p,0\downarrow}+R_{\pm\Delta k_f-p,0\uparrow}L_{p-\Delta k_f,\pi\downarrow}\\&\quad-L_{p,0\uparrow}R_{\Delta k_f(1\pm1)-p,\pi\downarrow}-R_{\Delta k_f(1\pm1)-p,\pi\uparrow}L_{p,0\downarrow}).\end{aligned}$$

Be careful that the symmetry of the 0 condensate is $d_{x^2-y^2}$ (i.e., it changes sign with $\tilde{C}$; see the definition afterwards), while that of the π condensate is both d_{xy} (i.e., it changes sign with p_x *and* p_y) and $d_{x^2-y^2}$; moreover, $d_{x^2-y^2}$ is imperfect on the π condensate [for instance, it maps a factor $\sin(a(p-k_{f0}+\Delta k_f/2))$ onto $\sin(a(-p-k_{f0}+\Delta k_f/2))$, which slightly differs]; however, the signs change according to g symmetry. A real space representation of the different condensate of singlet symmetry is given in Fig. 3.

If the components, in reciprocal variables, are multiplied by $\cos(mPa)$ (or some similar factor), one gets extended d condensates (this corresponds to the harmonic classification).

4. Triplet condensates

One also finds triplet instabilities.

$\Gamma=\delta_{i,i'\mp1}\delta_{jj'}$ corresponds to the p_x symmetry; $O_t^{(p_x)}(0)$ corresponds to an intraband pairing (0 condensate), and writes

$$\begin{aligned}O_t^{(p_x)}(0)&=\sum_i(\psi_{i,1\sigma}\psi_{i+1,1\sigma'}+\psi_{i,-1\sigma}\psi_{i+1,-1\sigma'})\tau^\alpha_{\sigma\sigma'}\\&\quad\sigma\sigma'\\&=-\mathrm{i}\int_L\frac{adp}{2\pi}\sum_{\sigma\sigma'}(L_{p,0\sigma}R_{-p,0\sigma'}\\&\quad+L_{p-\Delta k_f,\pi\sigma}R_{\Delta k_f-p,\pi\sigma'})\sin(a(p-k_{f0}))\tau^\alpha_{\sigma\sigma'}.\end{aligned}$$

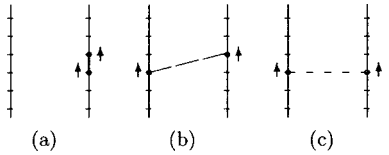

FIG. 4. Real space representation of SC condensate of triplet symmetry p_x (a), f_x (b), and f_y (c).

$O_t^{(p_x)}(\pi_\pm)$ corresponds to an interband pairing (π condensate), and writes

$$O_t^{(p_x)}(\pi_\pm) = -\mathrm{i}\sum_{i\sigma\sigma'} e^{\mp \mathrm{i}\Delta k_f i a}(\psi_{i,1\sigma}\psi_{i+1,1\sigma'} - \psi_{i,-1\sigma}\psi_{i+1,-1\sigma'})\tau^\alpha_{\sigma\sigma'}$$

$$= -e^{\pm \mathrm{i}(\Delta k_f a/2)}\int_L \frac{adp}{2\pi}\sum_{\sigma\sigma'}(L_{p,0\sigma}R_{\Delta k_f(1\pm1)-p,\pi\sigma'} + L_{p-\Delta k_f,\pi\sigma}R_{\pm\Delta k_f-p,0\sigma'})\sin(a(p - k_{f0} \mp \Delta k_f/2))\tau^\alpha_{\sigma\sigma'}.$$

Be careful that, because of the factor $e^{-\mathrm{i}Q_\perp jb/2}$ in the Fourier transform, this condensate is invariant under P.

With $\Gamma = \delta_{i,i'\mp1}\delta_{j,-j'}$, one gets an intraband pairing (0 condensate) of symmetry f_x, given by the $O_t^{(f_x)}(0)$ component

$$O_t^{(f_x)}(0) = \sum_{i\sigma\sigma'}(\psi_{i,1\sigma}\psi_{i+1,-1\sigma'} + \psi_{i,-1\sigma}\psi_{i+1,1\sigma'})\tau^\alpha_{\sigma\sigma'}$$

$$= \mathrm{i}\int_L \frac{adp}{2\pi}\sum_{\sigma\sigma'}(L_{p-\Delta k_f,\pi\sigma}R_{\Delta k_f-p,\pi\sigma'} - L_{p,0\sigma}R_{-p,0\sigma'})\sin(a(p-k_{f0}))\tau^\alpha_{\sigma\sigma'}.$$

Note that $d_{x^2-y^2}$ is again imperfect.

With $\Gamma = \delta_{i,i'}\delta_{j,-j'}$, one gets an interband pairing (π condensate) of symmetry f_y, given by the $O_t^{(f_y)}(\pi_\pm)$ component

$$O_t^{(f_y)}(\pi_\pm) = -\mathrm{i}\sum_{i\sigma\sigma'} e^{\mp \mathrm{i}\Delta k_f i a}(\psi_{i,1\sigma}\psi_{i,-1\sigma'} - \psi_{i,-1\sigma}\psi_{i,1\sigma'})\tau_{\sigma\sigma'}$$

$$= \mathrm{i}\int_L \frac{adp}{2\pi}\sum_{\sigma\sigma'}(L_{p,0\sigma}R_{\Delta k_f(1\pm1)-p,\pi\sigma'} - L_{p,\pi\sigma}R_{\Delta k_f(-1\pm1)-p,0\sigma'})\tau_{\sigma\sigma'}.$$

Note that p_y antisymmetry is an internal one and does not account on the exponential factor, in the Fourier transform. A real space representation of the different condensate of triplet symmetry is given in Fig. 4.

Extended states of the same symmetries can be obtained exactly the same way as for singlet superconducting operators.

B. Density wave instabilities

1. DW Hamiltonian

We have also investigated site density wave instabilities, defined by the order parameter $\Delta^{\mathrm{DW}}_{\mathrm{site}}(\mathbf{X}) = \Sigma_{\sigma\sigma'}\langle\psi^\dagger_{\mathbf{X},\sigma}\psi_{\mathbf{X},\sigma'}\rangle\tau^\alpha_{\sigma\sigma'}$, with $\tau^C = I$ for CDW, and $\tau^{S_x} = \sigma_x$, $\tau^{S_y} = \sigma_y$ and $\tau^{S_z} = \sigma_z$, for SDW, as well as bond density wave instabilities, defined by the order parameter $\Delta^{\mathrm{DW}}_{\mathrm{bond}}(\mathbf{X}) = \Sigma_{\sigma\sigma'}\langle\psi^\dagger_{\mathbf{X},\sigma}\psi_{\mathbf{X}+1_\parallel,\sigma'}\rangle\tau^\alpha_{\sigma\sigma'}$, where $\mathbf{1}_\parallel = (1,0)$. These couplings are intrachain, we distinguish intraband and interband ones. We also investigated interchain couplings, defined by the order parameters $\Delta^{\mathrm{DW}}_{\mathrm{site}}(\mathbf{X}) = \Sigma_{\sigma\sigma'}\langle\psi^\dagger_{\mathbf{X},\sigma}\psi_{\mathbf{X}+\mathbf{G},\sigma'}\rangle\tau^\alpha_{\sigma\sigma'}$ and $\Delta^{\mathrm{DW}}_{\mathrm{bond}}(\mathbf{X}) = \Sigma_{\sigma\sigma'}\langle\psi^\dagger_{\mathbf{X},\sigma}\psi_{\mathbf{X}+\mathbf{G}',\sigma'}\rangle\tau^\alpha_{\sigma\sigma'}$, where G or $G' \in \{\mathbf{1}_\perp, \mathbf{1}_\parallel + \mathbf{1}_\perp\}$ and $\mathbf{1}_\perp = (0,1)$.

The corresponding Hamiltonian writes, in reciprocal space variables,

$$H_{\mathrm{DW}} = \sum_{\substack{\mathbf{P}_1,\mathbf{P}_2\\ \sigma_1,\sigma_2}} \bar{\mathcal{Z}}^{\mathrm{DW}}(\mathbf{P}_1,\mathbf{P}_2,\mathbf{Q})\tau^{(\alpha)}\phi^\dagger_{\mathbf{Q}}\Psi^\dagger_{\mathbf{P}_1\sigma_1}\Psi_{\mathbf{P}_2\sigma_2} + \mathcal{Z}^{\mathrm{DW}}(\mathbf{P}_1,\mathbf{P}_2,\mathbf{Q})\bar{\tau}^{(\alpha)}\phi_{\mathbf{Q}}\Psi^\dagger_{\mathbf{P}_2\sigma_2}\Psi_{\mathbf{P}_1\sigma_1}. \quad (4)$$

The construction of the response functions for these instabilities is very similar to that of the superconducting instabilities. So, we will only give the Fourier components of the electron-hole pair operator for $\mathbf{Q} = (-2k_{f0}, 0)$, $\mathbf{Q} = (-2k_{f\pi}, 0)$, and $\mathbf{Q} = (-k_{f0} - k_{f\pi}, \pi/b)$.

SDW and CDW operators only differ by the spin factor (matrix σ or I), so we will also omit this factor.

2. DW response function

The intraband response functions write then

$$O_{\mathrm{site}}(-2k_{f0},0) = \int_L \frac{adp}{2\pi}R^\dagger_{p,0\sigma}L_{p,0\sigma'} + R^\dagger_{p+\Delta k_f,\pi\sigma}L_{p-\Delta k_f,\pi\sigma'},$$

$$O_{\mathrm{bond}}(-2k_{f0},0) = \mathrm{i}\int_L \frac{adp}{2\pi}\sin(ap)e^{-\mathrm{i}k_{f0}a}(R^\dagger_{p,0\sigma}L_{p,0\sigma'} + R^\dagger_{p+\Delta k_f,\pi\sigma}L_{p-\Delta k_f,\pi\sigma'})$$

and

$$O_{\mathrm{site}}(-2k_{f\pi},0) = \int_L \frac{adp}{2\pi}R^\dagger_{p-\Delta k_f,0\sigma}L_{p+\Delta k_f,0\sigma'} + R^\dagger_{p,\pi\sigma}L_{p,\pi\sigma'},$$

$$O_{\mathrm{bond}}(-2k_{f\pi},0) = \mathrm{i}\int_L \frac{adp}{2\pi}\sin(ap)e^{-\mathrm{i}k_{f\pi}a}(R^\dagger_{p-\Delta k_f,0\sigma}L_{p+\Delta k_f,0\sigma'} + R^\dagger_{p,\pi\sigma}L_{p,\pi\sigma'}).$$

The interband response function writes

$$O_{\mathrm{site}}\left(-k_{f0}-k_{f\pi},\frac{\pi}{b}\right) = \mathrm{i}\int_L \frac{adp}{2\pi}R^\dagger_{p,0\sigma}L_{p,\pi\sigma'} + R^\dagger_{p,\pi\sigma}L_{p,0\sigma'},$$

$$O_{\text{bond}}\left(-k_{f0}-k_{f\pi},\frac{\pi}{b}\right)=-\int_L \frac{adp}{2\pi}e^{ak_{f0}+k_{f\pi}/2}\sin(a(p-\Delta k_f/2))\times(R^{\dagger}_{p,\pi\sigma}L_{p,0\sigma'}+R^{\dagger}_{p+\Delta k_f,0\sigma}L_{p+\Delta k_f,\pi\sigma'}).$$

The above response functions are intrachain ones. The way we have written them one just needs to add a minus sign before the first (or second) term of all intrachain operators, to obtain all interchain ones.

IV. RENORMALIZATION GROUP EQUATIONS

A. Choice of the RG scheme

We have used the one particle irreducible (OPI) scheme (Refs. 26, 33, and 34), to calculate all diagrams, in a one-loop expansion. We use the flow parameter $\Lambda=\Lambda_o e^{-\ell}$. We do not renormalize v_f nor k_{f0} or $k_{f\pi}$.

B. $k_\parallel$-dependent equations

1. $k_\parallel$ dependence of the couplings

In this system, the interband backward scattering g_b plays a particular role. Due to momentum conservation, it is not possible to put all its arguments onto the Fermi points. This indicates that g_b is not a low energy process. However, it *intervenes* in the renormalization of low energy processes. For instance, in the renormalization of g_0, $dg_0/d\ell$ gives a contribution containing a g_{b0} scattering, with a factor $\Lambda/(\Lambda+v_f\Delta k_f)$. This contribution is exponentially suppressed, as $\Lambda \ll v_f\Delta k_f=2t_\perp$. It can thus be neglected as soon as $v_f\Delta k_f$ is of the order or bigger than the initial bandwidth $2\Lambda_0$. On the other hand, as shown by Fabrizio,[12] the g_b process has to be taken into account if $v_f\Delta k_f$ is much smaller than Λ_0.

Thereupon, in order to calculate the renormalization of g_{b0} properly, couplings g_0, g_f or g_t with specific $k_\parallel$ dependence are needed. For instance, $dg_{b0}/d\ell$ gives a Peierls diagram:

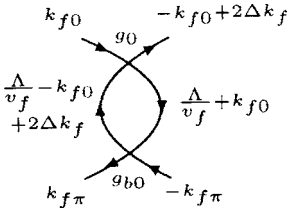

including coupling $g_0(k_{f0},-k_{f0}+2\Delta k_f,-k_{f0}+2\Delta k_f,k_{f0})$, with arguments that remain separated from the Fermi points, even in the limit $\Lambda\to 0$, let us write it g_{01}. This coupling separates from coupling $g_0(k_{f0},-k_{f0},-k_{f0},k_{f0})$, with all arguments at the Fermi points, which we will write g_{00}; therefore $k_\parallel$ dependence is influential. This can be proved by comparing their renormalization, in the Cooper channel. For instance, $dg_{00}/d\ell$ gives, in the Cooper channel, a term proportional to $g_0^2+g_t^2$ with a *constant* factor, which is present all the way down to $\Lambda\to 0$. On the contrary, $dg_{01}/d\ell$ gives, in the Cooper channel, a term with a factor $2\Lambda/(2\Lambda+v_f|P_1+P_2|)=\Lambda/(\Lambda+v_f\Delta k_f)$; the renormalization of g_{01} in the Cooper channel is thus exponentially suppressed, when $\Lambda\to 0$ (for g_{00}, the total incoming momentum is $P_1+P_2=0$).

We have proved that different g_0 couplings separate during the flow, so the $k_\parallel$ dependence is hence capable to have an effect during the flow, when it is taken into account. This generalizes for g_f, g_t and even g_b couplings.

All this differs completely from the one-dimensional case, where the renormalization of the coupling with all momenta on the Fermi points is only governed by processes with momenta $\pm k_f\pm\Lambda/v_f$, which always fall on the Fermi points when $\Lambda\to 0$. In our case, it is not possible to apply the same argument as soon as $t_\perp\ll\Lambda_o$. Indeed, we will see, in the following, that one gets different results, depending on whether we take the $k_\parallel$ dependence of the couplings into account or not.

The $k_\parallel$ dependence can be observed, when Λ is large (and until $\Lambda>v_f\Delta k_f$), by the separation of the different scattering couplings g_0, g_{f0} and g_{t0}. On the contrary, if one puts $g_b=0$ at $\ell=0$, this dependence is suppressed, and the system becomes purely one dimensional for small values of $t_\perp$ (in that case, g_b remains 0 for all Λ and the RG equations simplify drastically, although they differ from the one-dimension case).

2. $k_\parallel$ representation of the couplings g

In order to write explicit $k_\parallel$-dependent RG equations, one needs to define a consistent and detailed $k_\parallel$ representation of the couplings g.

Let us first note that $\mathcal{G}(P_1,P_2,P_2',P_1')$ corresponds to $R^{\dagger}(P_1)L^{\dagger}(P_2)L(P_2')R(P_1')$, where P_i are the absolute momenta in the $\parallel$ direction. We then define the relative momenta $p_1=P_1-k_{f\theta_1}$, $p_2=P_2+k_{f\theta_2}$, $p_3=P_3+k_{f\theta_3}$, and $p_4=P_4-k_{f\theta_4}$, and write, correspondingly, $g(p_1,p_2,p_2',p_1')$. We also introduce variables $c=p_1+p_2=p_1'+p_2'+d$, $l=p_1-p_1'=p_2'-p_2+d$, and $p=p_1-p_2'=p_1'-p_2+d$, where $d=-2\Delta k_f$ for g_{b0}, $d=2\Delta k_f$ for $g_{b\pi}$, and d is zero otherwise, and then write, correspondingly, $g(c,l,p)$ (d is implicit).

At the beginning of this section, we have found in a diagram a particular coupling $g_0(\Lambda/v_f,2\Delta k_f,0,2\Delta k_f+\Lambda/v_f)$. When $\Lambda\to 0$, we get $g_0(0,2\Delta k_f,0,2\Delta k_f)$ [which also writes $g_0(2\Delta k_f,-2\Delta k_f,0)$ in (c,l,p) notation]. Note that some arguments are shifted by $\pm 2\Delta k_f$, compared to the coupling $g_0(0,0,0,0)$ with all momenta on the Fermi points.

This could easily be generalized for all couplings g. So, in order to get a reasonable number of couplings, we have done the following approximation: all terms $\pm\Lambda/v_f$, in all diagrams, are replaced by their $2\Delta k_f$ part (i.e., by $2\Delta k_f[\Lambda/2\Delta k_f v_f]$, where $[x]$ is the biggest integer $\leqslant x$). Then, it follows that we only get couplings $g(p_1,p_2,p_2',p_1')$ [or $g(c,l,p)$], where all variables p_i (or c,l,p) are multiples of $2\Delta k_f$.

3. $k_\parallel$ representation of the couplings z

All the preceding procedures generalize to the couplings z as well. We first introduce a (k,c,p) representation, similarly, with $c=p_1+p_2$, $p=p_2-p_1$, and $k=p_1$, where p_1 and p_2 are defined in Fig. 19 and write, correspondingly, $z^{\text{SC}}(c,k)$ or $z^{\text{DW}}(p,k)$.

Then, we apply the same approximation in order to get couplings, where all variables (k,c,p) are multiples of $2\Delta k_f$.

The same conclusion applies to these couplings, proving that their $k_\parallel$ dependence is also influential.

4. RG equations

Finally, we calculate the RG flow of the separated following couplings: $g_0(0,0,0,0)$, $g_0(-2\Delta k_f,0,0,-2\Delta k_f)$, $g_0(0,2\Delta k_f,0,2\Delta k_f)$, etc. as well as $z(0,0)$, $z(2\Delta k_f,0)$, etc. The exact RG equations, including all $\parallel$ components, are given in Appendix B 1, for the $g(c,l,p)$, and in Appendix B 2, for the $z^{\mathrm{SC}}(c,k)$ and $z^{\mathrm{DW}}(p,k)$. In order not to solve an infinite number of equations, we have reduced the effective bandwidth of the renormalized couplings to $4n_{\max}\Delta k_f$, where $n_{\max}$ is an integer, by projecting all momenta lying out of the permitted band, back into it, according to a specific truncation procedure that will be explained after.

We have performed our calculations with $n_{\max}=2$, 3 or 4, and the results rapidly converge as $n_{\max}$ is increased.

5. Susceptibility equations

To each instability corresponds a susceptibility. We will write $\chi_\alpha^{\mathrm{SC}(\Gamma)}$ the different SC ones and $\chi_\alpha^{\mathrm{DW}}$ the different SDW or CDW ones. The susceptibilities have no $k_\parallel$ dependence. However, couplings z with *different* $k_\parallel$ variables appear in their RG equations, which we give in Appendix B 3.

Referring to the transverse component of the interaction vectors, we will write $\chi(0)$ the instabilities corresponding to intraband processes, and $\chi(\pi/b)$ those corresponding to interband ones. We use several symmetries, to reduce the number of couplings. Because of the $k_\parallel$ dependence, it is not as easy to apply them as in ordinary cases. We give here some indications, which are completed in the Appendixes.

C. Symmetries

1. Ordinary symmetries

We apply C the conjugation symmetry ($C:\mathbf{r}\to\mathbf{r}$, $\mathbf{p}\to-\mathbf{p},\sigma\to-\sigma$), A the (antisymmetrical) exchange between incoming particles, A' the exchange between outgoing particles, P the space parity ($P:\mathbf{r}\to-\mathbf{r},\mathbf{p}\to-\mathbf{p},\sigma\to\sigma$), and S the spin rotation ($S:\sigma\to-\sigma$). We will also use p_x, p_y (the mirror symmetries in the $\parallel$ and $\perp$ directions), f_x and f_y. Note that $P=p_xp_y$.

H_{cin} [Eq. (1)] and H_{int} [Eq. (2)] satisfy all these symmetries, whereas SC instabilities, governed by H_{SC} [Eq. (3)], are not invariant under S or C, which allows a natural classification of the states, and DW instabilities, governed by H_{DW} [Eq. (4)], do satisfy CS, AS or $A'S$, but not C, A, A', nor S symmetries.

All the relations satisfied by $\mathcal{G}$ or $\mathcal{Z}$ couplings are detailed in Appendix C 1. From what precedes, one will not be surprised that those for $\mathcal{G}$ couplings are simpler and less sophisticated than those for $\mathcal{Z}$ ones.

Relations of couplings g. We are not interested here in the symmetries that relate, for instance, a *LRLR* coupling to a *RLLR* one. Instead, we only keep *RLLR* couplings and deduce all the symmetries that keep this order.

We then apply them to every coupling g_0, g_π, etc., and find, altogether, exactly two independent relations for each one, which write, in (c,l,p) notation,

$$g_i(c,l,p)=g_i(-c,l,p)\quad i=0,\pi,t0,t\pi,$$

$$g_{f\pi}(c,l,p)=g_{f0}(-c,l,p),$$

$$g_{b\pi}(c,l,p)=g_{b0}(-c,l-2\Delta k_f,p-2\Delta k_f), \tag{5}$$

$$g_i(c,l,p)=g_i(c,-l,p)\quad i=0,\pi,f0,f\pi,$$

$$g_{t\pi}(c,l,p)=g_{t0}(c,-l,p),$$

$$g_{b\pi}(c,l,p)=g_{b0}(c-2\Delta k_f,-l,p-2\Delta k_f). \tag{6}$$

One observes that (5) relates g_{f0} to $g_{f\pi}$ and g_{b0} to $g_{b\pi}$, while (6) relates g_{t0} to $g_{t\pi}$ and g_{b0} to $g_{b\pi}$. The combination of (5) and (6) thus relates g_{f0} to $g_{f\pi}$ and g_{t0} to $g_{t\pi}$.

Relations of couplings z. We similarly deduce all symmetries that keep the *LR* order; we apply them to every coupling z_0, z_π, etc., and find only one relation for each one, which writes, in (k,c,p) notation,

$$z_{s\theta}^{\mathrm{SC}}(c,k)=z_{s\theta}^{\mathrm{SC}}(-c,k-c)\quad\theta=0,\pi,$$

$$z_{t0}^{\mathrm{SC}}(c,k)=z_{t\pi}^{\mathrm{SC}}(-c,k-c),$$

$$z_{s-}^{\mathrm{SC}}(c,k)=\pm z_{s+}^{\mathrm{SC}}(-c,k-c),$$

$$z_{t-}^{\mathrm{SC}}(c,k)=\pm z_{t+}^{\mathrm{SC}}(-c,k-c), \tag{7}$$

where $\pm$ reads $+$ for $\Gamma=s$ or $\Gamma=p_x$ and $-$ for $\Gamma=g$ or $\Gamma=f_y$. Note that z_0^{SC} or s_π^{SC} correspond to intraband condensates, while z_+^{SC} or s_-^{SC} correspond to interband ones.

$$z_\theta^{\mathrm{DW}}(p,k)=\pm z_\theta^{\mathrm{DW}}(p,-p-c)\quad\theta=0,\pi,$$

$$z_-^{\mathrm{DW}}(p,k)=\pm z_+^{\mathrm{DW}}(p,-p-c), \tag{8}$$

where $\pm$ reads $+$ for site ordering and $-$ for bond ordering.

One observes that (7) and (8) relate z_+ to z_-.

2. Supplementary symmetry

As we already noted, ordinary symmetries do not relate g_0 to g_π, nor z_0 to z_π. However, since we choose identical bare values at $\ell=0$, and since the RG equations are symmetrical, we observe an effective symmetry between these couplings: we will show here that this does not occur by chance, but that it follows a specific symmetry $\tilde{C}$, which only applies to the ladder system.

$\tilde{C}$ is a kind of conjugation: it generalizes the electron-hole symmetry as follows.

Let us first consider the case of a single band one-dimensional system; we find an electron-hole symmetry, described in Fig. 5(a).

For R particles, it conjugates an electron with momentum k_f+p and a hole with momentum k_f-p. In the momentum space, it is a symmetry around k_f. One can write $\tilde{C}\psi_p=\psi_{2k_f-p}^\dagger$ and $\tilde{C}\psi_p^\dagger=\psi_{2k_f-p}$. For L particles, the same relation applies if one simply changes k_f into $-k_f$.

Let us now return to the two-band system. This symmetry generalizes by turning the momenta around the isobarycenter

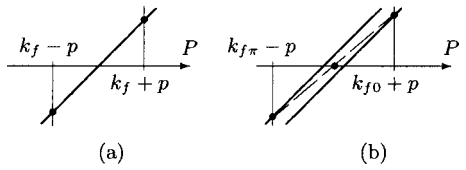

FIG. 5. Symmetry around the Fermi points: (a) in a 1-band system; (b) in a 2-band system

of the Fermi points, as shown in $\|$ space in Fig. 5(b). For R particles, $(k_{f0}+k_{f\pi})/2$ points to the isobarycenter and you now get $\tilde{C}\psi_p=\psi^\dagger_{k_{f0}+k_{f\pi}-p}$ etc.

In the two-dimensional representation, $\tilde{C}$-symmetry is a point symmetry around $(\pm(k_{f0}+k_{f\pi})/2, \pi/2b)$, as shown in Fig. 2 (the sign depends on whether it is a R or L momentum).

Actually, there is an alternative symmetry, which we write $\mathcal{C}$, which also maps the band $k_\perp=0$ onto the band π: it is a translation by the vector $[\pm(k_{f\pi}-k_{f0}), \pi/b]$, as shown in Fig. 2. Some of the bare couplings satisfy this $\mathcal{C}$ symmetry (g_0, g_f, g_t, z_0 or z_π), but some do not (g_b, z_+, z_-). Since interactions are mixing all couplings as soon as the flow parameter $\ell>0$, the renormalized couplings will break the $\mathcal{C}$ symmetry. Therefore, we cannot use it.

On the contrary, one verifies that $H_{\rm cin}$, $H_{\rm int}$, $H_{\rm SC}$ and $H_{\rm DW}$ are invariant under $\tilde{C}$. The induced relations satisfied by $\mathcal{G}$ or $\mathcal{Z}$ couplings are detailed in Appendix C 2.

In fact, $\tilde{C}$ and $\mathcal{C}$ weakly correspond to the $d_{x^2-y^2}$ symmetry in two dimensions.

Supplementary relation of couplings g. It is straightforward that $\tilde{C}$ keeps the *RLLR* order when one applies it to any coupling g_i; so we find a new relation for each one, which writes, in (c,l,p) notation,

$$g_\pi(c,l,p) = g_0(-c,-l,-p),$$

$$g_{f\pi}(c,l,p) = g_{f0}(-c,-l,-p),$$

$$g_{t\pi}(c,l,p) = g_{t0}(-c,-l,-p),$$

$$g_{b\pi}(c,l,p) = g_{b0}(-c,-l,-p). \tag{9}$$

One verifies that g_0 and g_π are related; in fact, (9) relates all 0 couplings to π couplings.

Supplementary relation of couplings z. Similarly, $\tilde{C}$ keeps *LR* order when we apply it to any coupling z_i; so we find a new relation for each one, which writes, in (k,c,p) notations,

$$z^{\rm SC}_\pi(c,k) = \pm z^{\rm SC}_0(-c,-k),$$

$$z^{\rm SC}_-(c,k) = \pm z^{\rm SC}_+(-c,-k), \tag{10}$$

where $\pm$ reads $+$ for $\Gamma=s$ or $\Gamma=p_x$ and $-$ for $\Gamma=d$, g or $\Gamma=f_x, f_y$,

$$z^{\rm DW}_\pi(p,k) = \pm z^{\rm DW}_0(-p,-k),$$

$$z^{\rm DW}_-(p,k) = \pm z^{\rm DW}_+(-p,-k), \tag{11}$$

where $\pm$ reads $+$ for site ordering and $-$ for bond ordering.

Again, one verifies that z_0 and z_π are related (as well as z_+ and z_-).

D. Truncation

Understanding symmetry relations does not only help us to reduce drastically the number of couplings, it is also an essential tool to make a proper truncation procedure, as we will explain now.

1. Triplet notation

Let us first introduce a useful notation for the $k_\|$ dependence.

We have already defined the relative momentum representation $g(p_1,p_2,p_2',p_1')$, as well as the $g(c,l,p)$ notation, and explained how to keep only couplings, the arguments of which are all multiples of $2\Delta k_f$. We will focus on the (c,l,p) notation and write $c=2n_1\Delta k_f$, $l=2n_2\Delta k_f$, $p=2n_3\Delta k_f$, with $(n_1,n_2,n_3)\in\mathbb{Z}^3$.

In short, we can write $g_i(n_1,n_2,n_3)$ $(i=0,f0,t0,b0)$, where (n_1,n_2,n_3) is called a triplet. Mind that, using symmetry relations, two triplets (n_1,n_2,n_3) and (n_1',n_2',n_3') can represent the same coupling. One says that these triplets belong to the same symmetry orbit (or symmetry class). Mind also that the orbits are different for each coupling g_0, g_{f0}, g_{t0}, and g_{b0}.

It would take too long to give an exhausted list of these orbits. Let us just observe that (0,0,0)'s orbit has only one element (itself), except for g_b, the orbits of which we detailed in Appendix C 3.

2. Choice of the truncation procedure

Obviously, one needs only renormalize one coupling per orbit. From the fundamental rules, explained in Sec. IV B 2, it follows that, even if one starts with only $g_0(0,0,0)$, $g_{f0}(0,0,0)$, and $g_{t0}(0,0,0)$, the RG equations will generate an infinite number of orbits. So, we will only keep couplings which satisfy $|n_i|\leqslant n_{\max}$ (for a given $n_{\max}$); but even so, in the RG equations of some orbits intervene couplings, with arguments lying outside of the permitted band (i.e., the distance of the corresponding momentum to the Fermi point exceeds $2n_{\max}\Delta k_f$). In order to get a consistent closed set of differential equations, one needs to put these extra couplings back, inside the set of allowed couplings.

For instance, imagine that $n_{\max}=2$, and that $g(3,2,2)$ coupling intervenes in a RG equation. One cannot, unfortunately, just map $(3,2,2)\mapsto(2,2,2)$, because these triplets *do not belong to the same symmetry orbit*. In doing so, one would get a very poor $k_\|$ dependence; we have actually proved, in the case of a (p_1,p_2,p_2') representation, that all orbits of g_0 except (0,0,0) would collapse into one single orbit.

Therefore, the truncation procedure *must be* compatible with all the symmetries of the system. We have used the (c,l,p) notation, which is very convenient. One can check

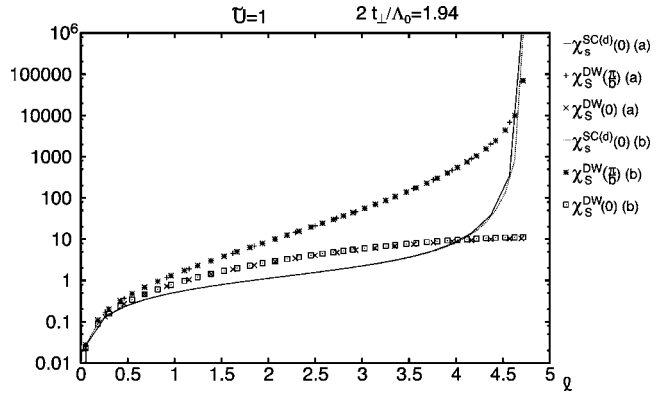

FIG. 6. Flow of the susceptibilities $\chi_s^{\mathrm{SC}(d)}$ and χ_S^{DW} (intra or interband), at $\tilde{U}=1$ and $2t_\perp/\Lambda_0=1.94$: (a) usual RG procedure; (b) including $k_\parallel$ dependence. You observe that $\chi_S^{\mathrm{DW}}(0)$ does not diverge but only reaches a plateau.

that all the symmetries conserve $c+l+p$ modulo $4\Delta k_f$. This explains why $n_i \mapsto n_i \pm 1$ cannot be compatible with the symmetries. On the contrary, $n_i \mapsto n_i \pm 2$ is completely compatible, i.e., it maps a triplet onto on an already defined orbit; hence we have used this mapping for the extra couplings.

With $n_{\max}=2$, for each coupling g we find 63 different couplings [that are $\{(i,j,k),i,j,k=-2,0,2\} \cup \{(\pm 1,\pm 1,i), i=-2,0,2\} \cup \{(\pm 1, i, \pm 1), i=-2,0,2\} \cup \{(i, \pm 1, \pm 1), =-2,0,2\}$], which separate into 23 orbits (having 1, 2, or 4 elements), except for the g_b couplings. For these, the enumeration is more tedious, we eventually find 8 orbits (of 4 elements, see Appendix C 3). There are altogether $3\times 23+8=77$ different orbits; if we include the spin separation, we thus need to calculate 154 coupled differential equations. $n_{\max}=3$ gives 390, while $n_{\max}=4$ gives 806.

E. Divergences of the susceptibilities

In the range of values for U that we have investigated, the RG flow is always diverging.

When the initial interaction Hamiltonian H_{int} is purely local, i.e., when the interchain scatterings are discarded ($C_{\mathrm{back}}=C_{\mathrm{for}}=0$), the interband SDW susceptibility $\chi_S^{\mathrm{DW}}(\pi/b)$ is always divergent. In the superconducting phase, the SC singlet d susceptibility $\chi_s^{\mathrm{SC}(d)}(0)$ is also divergent, at the same critical scale $\Lambda_c=\Lambda_0 e^{\ell_c}$. A third susceptibility $\chi_S^{\mathrm{DW}}(0)$ increases and reaches a high plateau (see Fig. 6). Almost all other susceptibilities remain negligible.

When the parameters C_{back} or C_{for} are increased, both $\chi_S^{\mathrm{DW}}(\pi/b)$ and $\chi_s^{\mathrm{SC}(d)}$ decrease; they are progressively replaced by the divergence of the CDW susceptibility $\chi_C^{\mathrm{DW}}(\pi/b)$, and, in the case of backward scattering, of the triplet SC susceptibility $\chi_t^{\mathrm{SC}(f)}(0)$.

One finds at most four divergent susceptibilities [$\chi_s^{\mathrm{SC}(d)}(0)$, $\chi_C^{\mathrm{DW}}(\pi/b)$, $\chi_t^{\mathrm{SC}(f)}(0)$, and $\chi_S^{\mathrm{DW}}(\pi/b)$] at a time.

Since the RG flow is diverging, we cannot further calculate the renormalized couplings. To deduce a phase diagram, we must find out which mechanism dominates; we used two different criteria: according to the first one, we simply take the susceptibility which reaches the highest value $|\chi|$ at Λ_c; according to the second one, we take the susceptibility which has the highest slope.

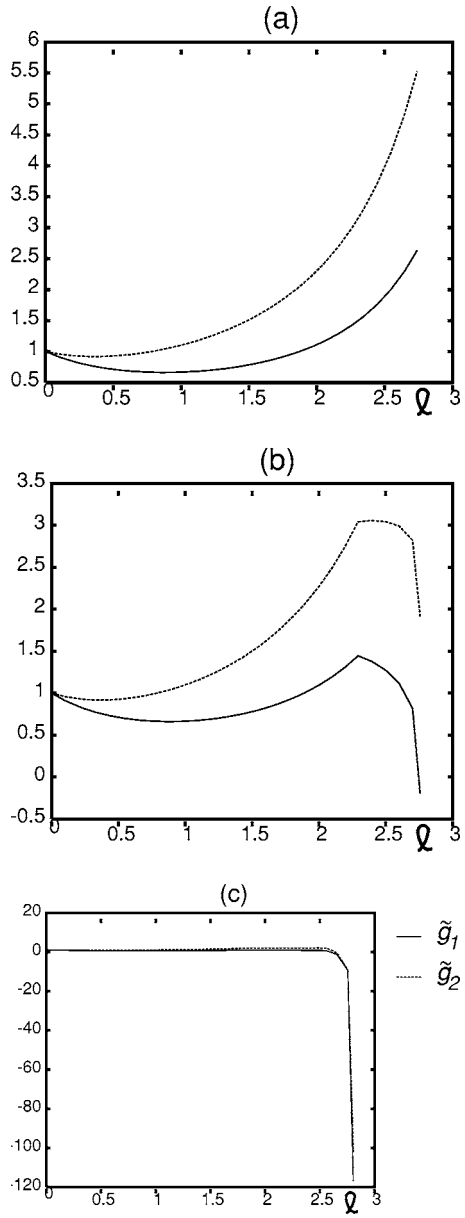

FIG. 7. Flow of the couplings $\tilde{g}_{01}$ and $\tilde{g}_{02}$ at (a) $t_\perp \lesssim t_{\perp c}(U)$, (b) $t_\perp = t_{\perp c}(U)$, and (c) $t_\perp \gtrsim t_{\perp c}(U)$.

These two criteria bring nonequal results. Although the first one is a poorer criterion, its conclusions remain stable when either the precision or $n_{\max}$ are changed. The second is however preferred, as we will see its conclusions are physically consistent, contrary to the first one.

V. PHASE DIAGRAM WITH INITIALLY LOCAL INTERACTIONS

Let us first discuss the case of initially local interactions ($C_{\mathrm{back}}=C_{\mathrm{for}}=0$, no interchain scattering). Of course, we can only fix H_{int} at $\ell=0$, and the flow will develop nonlocal interactions.

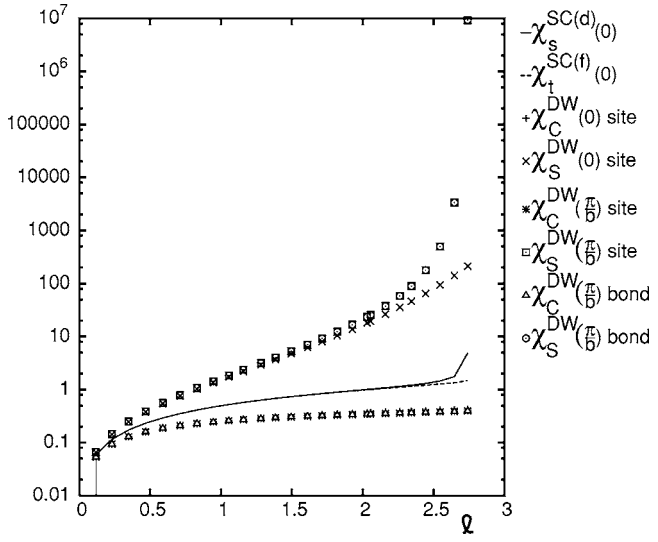

FIG. 8. Flow of some susceptibilities, at $\tilde{U}=1$ and $2t_\perp/\Lambda_0=0.016$. $\chi_s^{SC(d)}(0)$ is almost suppressed at Λ_c.

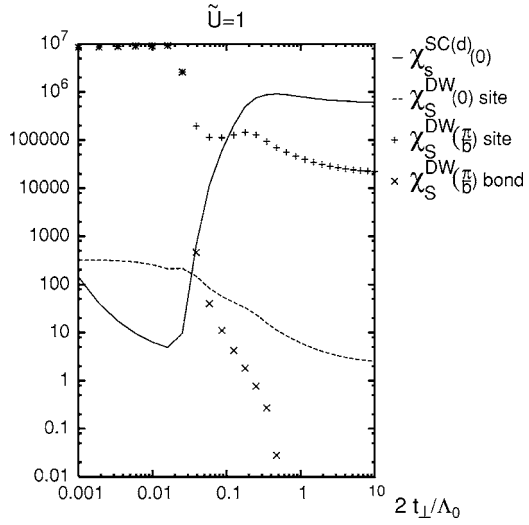

FIG. 9. Curves of $\chi_s^{SC(d)}(\Lambda_c)$ and $\chi_S^{DW}(\Lambda_c)$ versus $2t_\perp/\Lambda_0$.

A. Results

We begin with the phase diagram obtained when the $k_\parallel$ dependence is neglected.

1. Phase diagram with no $k_\parallel$ dependence

In the region of the phase diagram that we have investigated ($0\leqslant\tilde{U}\leqslant 2$), the SC susceptibility $\chi_s^{SC(d)}(0)$ is always divergent, as well as the SDW susceptibility $\chi_S^{DW}(\pi/b)$ (see Fig. 6).

According to the slope criterion, $\chi_s^{SC(d)}(0)$ always dominates. We induce that this region is superconducting (this is consistent with the conclusions of Fabrizio[12]), and that the pairing is of symmetry *d*; however, the presence of SDW instabilities, developing in the same region, makes a detailed determination of this phase very uneasy and beyond the possibilities of our approach. We will call it SC phase.

2. Phase diagram with $k_\parallel$ dependence

SC phase. When $t_\perp$ is large, we find similar results. For instance, with $\tilde{U}=1$, there are no significant differences for $2t_\perp/\Lambda_0\geqslant 1.94$ (see Fig. 6).

SDW phase. On the contrary, the superconducting susceptibility is almost suppressed when $t_\perp$ is small enough. For $\tilde{U}=1$ and $2t_\perp/\Lambda_0=0.016$, $\chi_s^{SC(d)}(0)$ is 5 orders of magnitude smaller than $\chi_S^{DW}(\pi/b)$, at Λ_c; see Fig. 8. In this phase, the SDW's instability develops so rapidly that it overwhelms all other processes. This indicates indeed a pure SDW phase.

Hence, this result differs drastically from those obtained when the $k_\parallel$ dependence is neglected.

Moreover, we observe a transition between the SDW phase and the SC one, at a critical parameter $t_{\perp c}(U)$.

Critical behavior. We characterize this transition in different ways.

First of all, the behavior of the renormalized two-particle couplings changes very rapidly, at $t_{\perp c}(U)$: as $t_\perp$ decreases, $|\tilde{g}_{01}(\Lambda_c)|$ and $|\tilde{g}_{02}(\Lambda_c)|$ shrink suddenly, then, after a little interval, $\tilde{g}_{01}(\Lambda_c)$ and $\tilde{g}_{02}(\Lambda_c)$ become positive (and even $>\tilde{U}$; see Fig. 7). We also observe changes, though less significant, for the other couplings $\tilde{g}$ [for instance, $|\tilde{g}_{f01}(\Lambda_c)|$ decreases and $\tilde{g}_{b1}(\Lambda_c)$ becomes negative when $t_\perp$ increases].

Moreover, we observe (in Fig. 9) a marked site or bond separation of the SDW susceptibility, at $t_{\perp c}(U)$. The site and bond SDW susceptibilities are degenerate for $t_\perp\leqslant t_{\perp c}(U)$ (in the SDW phase), which is consistent with the fact they should be equal at $t_\perp=0$ (where the system is purely one-dimensional, see Ref. 35), while they smoothly separate after the transition. The same site or bond separation occurs for the CDW susceptibility.

Transition region. The behavior of most of the parameters that we have examined indicates the same critical value $t_{\perp c}(U)$, which we have determined exactly, using the slope criterion.

However, $|\chi_s^{SC(d)}(0)|<|\chi_S^{DW}(\pi/b)|$ holds until $t_\perp$ reaches a value $t_{\perp c2}(U)$; this second critical value, which corresponds to the height criterion, is confirmed by minor modifications of behavior, which occur in the interval $t_{\perp c}(U)<t_\perp\leqslant t_{\perp c2}(U)$ and are very smooth [for instance, $\tilde{g}_{b1}(\Lambda_c)$ and $\tilde{g}_{b2}(\Lambda_c)$ cross].

The numerical determination of $t_{\perp c2}(U)$ is very stable (see Fig. 10), and the complete behavior, from the SDW phase to the SC phase, is clear on Fig. 9, which shows the absolute values of the susceptibilities at Λ_c.

The region $t_{\perp c}(U)<t_\perp\leqslant t_{\perp c2}(U)$ is called transition region; we believe it is a superconducting phase, where SDW instabilities seem however to dominate. The SDW are precursor manifestations of the pure SDW phase, which is next to the transition region.

As already stated, our results converge very rapidly when the band width on which we project the momenta is increased. The complete phase diagram (for $C_{\text{back}}=C_{\text{for}}=0$) is shown in Fig. 10, for $n_{\max}=2$, 3, and 4.

Moreover, it is most interesting to note that, contrary to the pure SDW phase, the transition region can be detected when the $k_\parallel$ dependence is neglected [the value of $t_{\perp c2}(U)$ is

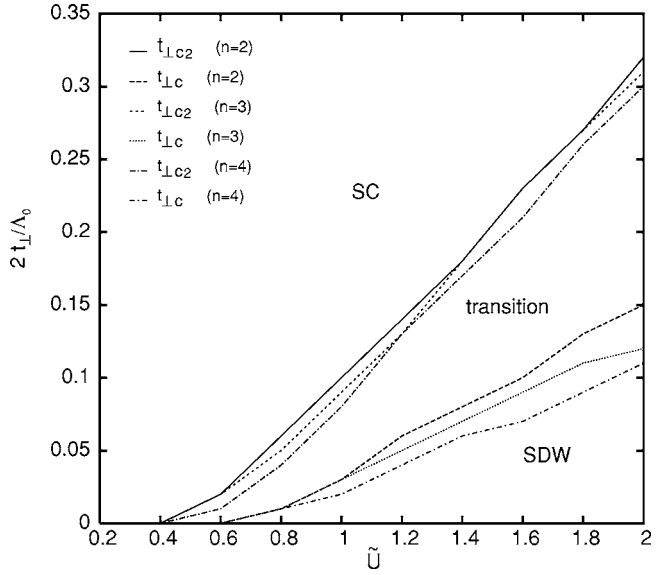

FIG. 10. Phase diagram when the $k_\parallel$ dependence is included.

lowered]. This can be seen, for instance, in Fig. 11, which corresponds to Fig. 9 with no $k_\parallel$ dependence.

SC critical temperature. The critical energy Λ_c at which SC susceptibility diverges gives an approximate indication of the SC critical temperature. We give a plot of Λ_c/Λ_0 versus $2t_\perp/\Lambda_0$; as seen in Fig. 12, Λ_c is roughly decreasing with $t_\perp$. The band gap parameter $t_\perp$ is also increasing with pressure; therefore, this behavior is compatible with the experimental data, which show that T_c is decreasing with pressure in quasi-one-dimensional organic compounds.

B. Discussion

As already mentioned, as soon as the dependence of $k_\parallel$ is included, we observe two separated phases, one purely SDW,

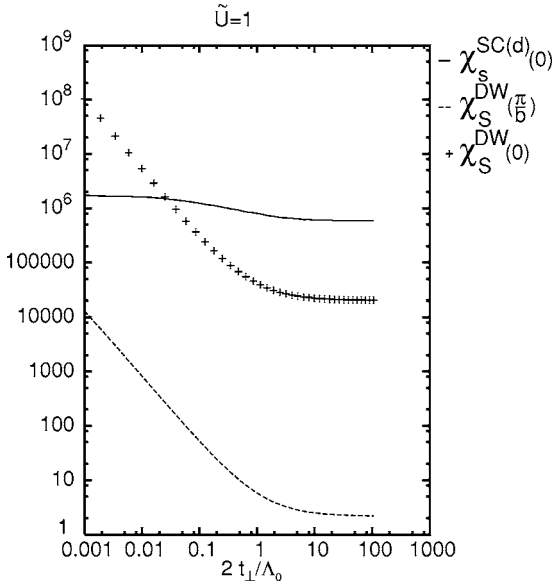

FIG. 11. Curves of $\chi_s^{(d)}(\Lambda_c)$ and $\chi_S^{\mathrm{DW}}(\Lambda_c)$ versus $2t_\perp/\Lambda_0$ when $k_\parallel$ is neglected.

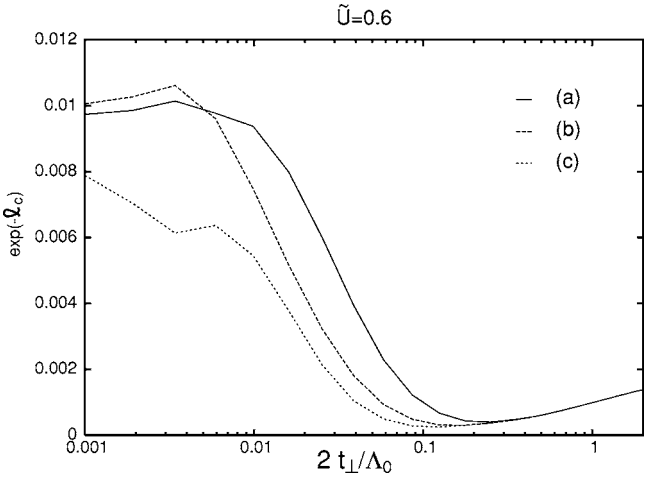

FIG. 12. Curves of $\Lambda_c/\Lambda_0=e^{-\ell_c}$ versus $2t_\perp/\Lambda_0$ with $n_{\max}=2$ (a), $n_{\max}=3$ (b), and $n_{\max}=4$ (c).

the other one a SC phase with competing SDW instabilities.

On the other hand, for $t_\perp \geqslant 1$, i.e., when the initial bandwidth lies inside $[k_{f\pi}, k_{f0}]$, the $k_\parallel$ dependence has no observable influence on the susceptibilities.

In the SDW phase, our results prove the existence of large antiferromagnetic fluctuations. We believe that these SDW instabilities are not the signature of a localized antiferromagnetic ground state, but of antiferromagnetic itinerant electrons, as it is indeed observed in Bechgaard salts. Actually, the flow is driving towards a fixed point, which does not seem to be the one-dimensional solution: for instance, the renormalized couplings $\tilde{g}_1$ and $\tilde{g}_2$ of the 1D solution are 0 and 1/2 and differ from the values which we obtain when the flow is diverging, in the SDW phase [see Fig. 7(a)].

We induce that the spin-gap should disappear in this SDW region, which is consistent with what Park and Kishine[23,24] claim.

In the SC phase, the SC divergence is due to the Cooper channel, while that of density waves is due to the Peierls one (see, in the case of a single band model, Refs. 32 and 36). The appearance of *d*-wave superconductivity in ladder systems is well understood within a strong coupling scenario, where a spin gap leads to interchain Cooper pairing. However, in our calculations, we see that superconducting correlations are always enhanced by SDW fluctuations. Contrary to what Lee *et al.* claimed first,[37] there is an itinerant electron mechanism in this case, which is the weak coupling equivalent of the localized electron mechanism in the strong electron scenario. It was proposed by Emery,[38] and is essentially the spin analog of Kohn-Luttinger superconductivity. The mutual enhancement of the two channels is also discussed in Refs. 33 and 39.

As a consequence of this mutual enhancement, the spin-gap should not appear with the first appearance of SC instabilities, but for somehow larger values of $t_\perp$.

Moreover, we observe that the SC pairing is a $\mathbf{Q}=\mathbf{0}$ mechanism, while the SDW are excited by $\mathbf{Q}=(2\Delta k_f, \pi/b)$ vectors. This can be explained by the symmetry of each channel. The Green function of the Cooper channel gives a factor $1/[\epsilon(\mathbf{k})+\epsilon(-\mathbf{k})]$ and is minimized with the $\mathbf{k}\mapsto-\mathbf{k}$

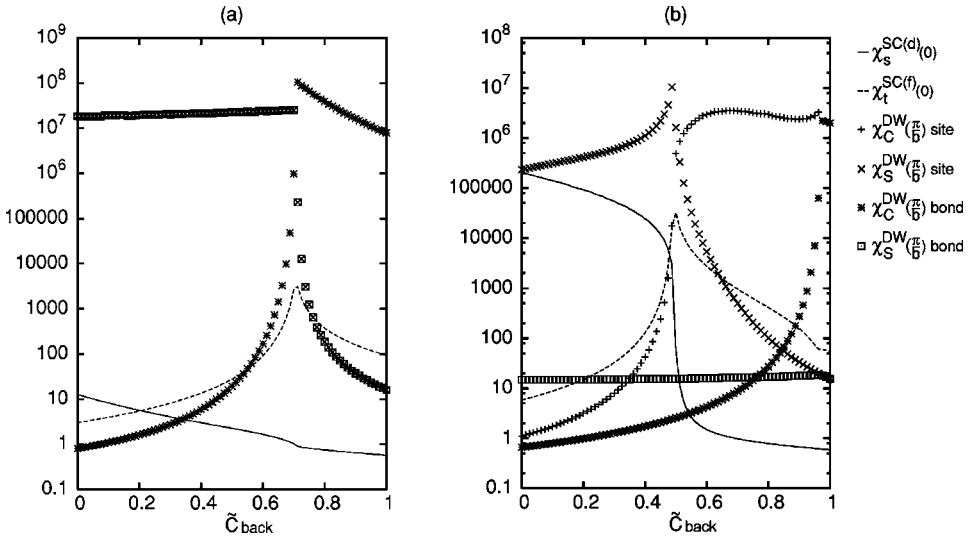

FIG. 13. Curves of the $\chi(\Lambda_c)$ versus $\tilde{C}_{\text{back}}$, at $\tilde{U}=1$ and (a) $2t_\perp/\Lambda_0=0.01$; (b) $2t_\perp/\Lambda_0=0.1$.

symmetry, which corresponds to an intraband process. The Green function of the Peierls channel gives a factor $1/[\epsilon(\mathbf{k})+\epsilon(\mathbf{k}+\mathbf{Q})]$ and is minimized with the $\mathbf{k}\mapsto\mathbf{k}+\mathbf{Q}$ symmetry, which corresponds to an interband process.

This can also be seen in the RG equations. $d\ln(z^{\text{SC}}(0))/d\ell$ depends only on g_0 and g_t, whereas $d\ln(z^{\text{SC}}(\pi/b))/d\ell$ depends on g_f and g_b. Since g_b processes are depressed as soon as $\Lambda\leqslant 2t_\perp$, 0 condensate are favored. Moreover, this predominance is stabilized by the $dg_t/d\ell$ equations, in which the Cooper term depends on g_0, and by the $dg_b/d\ell$ equations, in which the Cooper term depends on g_f.

The same argument applies for DW instabilities. $d\ln(z^{\text{DW}}(0))/d\ell$ depends on g_0 and g_b, whereas $d\ln(z^{\text{DW}}(\pi/b))/d\ell$ depends on g_f and g_t. So, π processes are favored. Again, this is stabilized by the $dg_t/d\ell$ equations, in which the Peierls term depends on g_f, and by the $dg_b/d\ell$ equations, in which the Peierls term depends on g_0.

The critical temperature, in the SC phases, is indicated in Fig. 12. We chose $\tilde{U}=0.6$ in order to avoid the SDW phase. The general trend is that of a quasi-one-dimensional system; the increasing curve, for small values of $t_\perp$, can be related to transition effect and to the furthered influence of the SDW fluctuations.

VI. PHASE DIAGRAM WITH INITIAL COULOMBIAN INTERCHAIN SCATTERING

A. Results

1. Influence of a backward interchain scattering

Let us now study the effect of a backward interchain scattering. This type of coupling has been investigated by Bourbonnais *et al.*[29] in the context of correlated quasi-one-dimensional metals, for which CDW correlations are enhanced and triplet superconducting instabilities can occur. When the parameter $\tilde{C}_{\text{back}}$ is increased, the behavior of the susceptibilities depends on the parameters $(t_\perp,\tilde{U})$.

Appearance of triplet SC and CDW. For $t_\perp\leqslant t_{\perp c}(U)$, the SDW phase exists for $\tilde{C}_{\text{back}}$ small enough. As $\tilde{C}_{\text{back}}$ is further increased, the SDW instabilities are replaced by CDW ones. The transition is smooth, and there is a narrow region where both SDW and CDW coexist (region 3 in Fig. 16). We show a $2t_\perp/\Lambda_0=0.01$ section of the susceptibilities at Λ_c in Fig. 13.

For $t_\perp\geqslant t_{\perp c}(U)$, the SC phase (with SC singlet d and SDW instabilities) exists for $\tilde{C}_{\text{back}}$ small enough. As $\tilde{C}_{\text{back}}$ is further increased, the singlet SC modes are replaced by triplet ones, while SDW are replaced by CDW. Singlet and triplet SC appear to be antagonistic, and the transition is very pronounced; in the coexistence line between them, one also finds SDW and CDW divergences (see Fig. 14). On the contrary, the transition between SDW and CDW is very smooth, although the coexistence region is still narrow (region 2 in Fig. 16). We show a $2t_\perp/\Lambda_0=0.1$ section of the susceptibilities at Λ_c on Fig. 13.

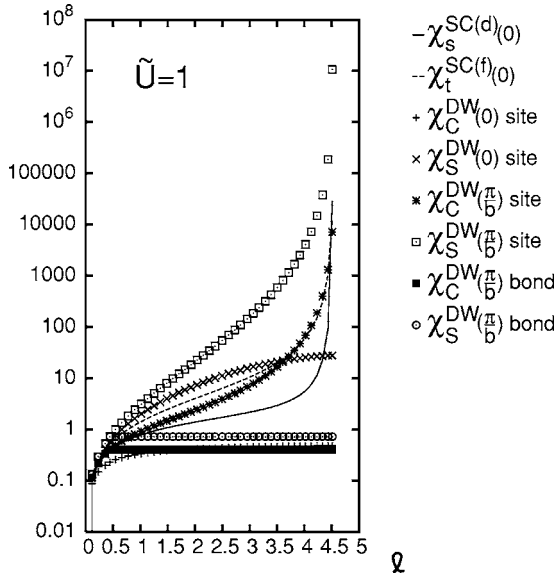

FIG. 14. Flow of the susceptibilities for $2t_\perp/\Lambda_0=0.32$ and $\tilde{C}_{\text{back}}=0.18$.

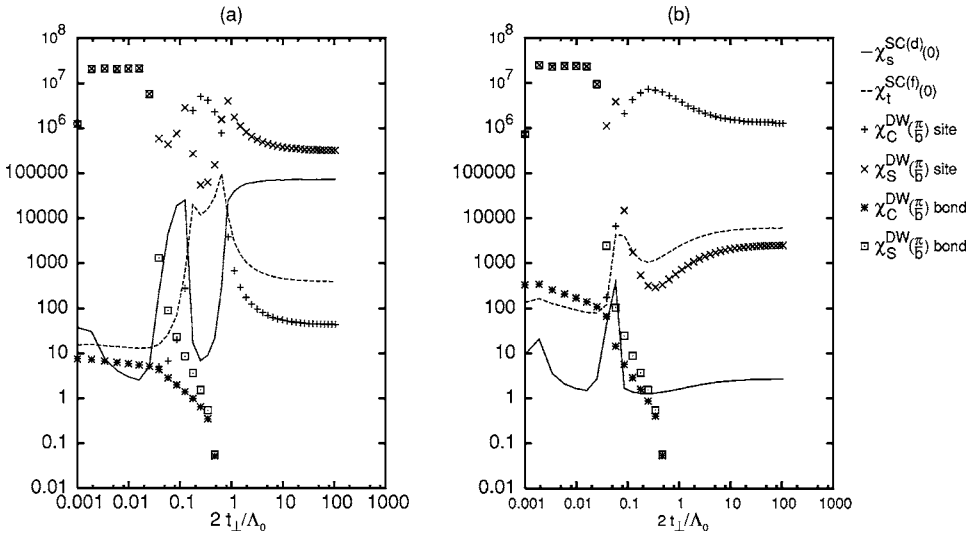

FIG. 15. Curves of the susceptibilities $\chi(\Lambda_c)$ versus $2t_\perp/\Lambda_0$, for (a) $\tilde{C}_{\text{back}}=0.4$; (b) $\tilde{C}_{\text{back}}=0.6$.

The triplet SC condensate has f_x symmetry. The corresponding susceptibility is mostly divergent in a region of coexistence with SDW and CDW (region 2 in Fig. 16), but it is also divergent in a region of coexistence with only CDW (region 1 in Fig. 16).

When $\tilde{C}_{\text{back}}$ is large enough, the triplet SC modes are suppressed, and the region is a pure CDW phase. We show a section of the susceptibilities at Λ_c, for $\tilde{C}_{\text{back}}=0.2$ and $\tilde{C}_{\text{back}}=0.3$, on Fig. 15, which clearly indicates the domain of existence of the triplet SC.

Site or bond separation. As we have already observed it, in the case of $C_{\text{back}}=C_{\text{for}}=0$, for small values of $t_\perp$, site and bond SDW susceptibilities are degenerate, as well as site and bond CDW ones.

This generalizes for all values of $\tilde{C}_{\text{back}}$. The site or bond separation line is an increasing function $t_{\perp g}(C_{\text{back}})$ of C_{back}, shown in Fig. 16; For small values of U, this line crosses the SC domain, but for $\tilde{U}=1$ it is already disconnected from the SC frontier (although it remains close to it).

2. Influence of a forward interchain scattering

The phase diagram when C_{for} is included is very rich, and beyond the scope of this article.

We would like to emphasize only the fact that all SC instabilities are suppressed when C_{for} is increased. Figure 17 gives a typical flow of the susceptibilities, with a large $\tilde{C}_{\text{for}}$.

B. Discussion

Let us analyze these behaviors, which follow simple trends.

The CDW instabilities are enhanced when g_C is increased, whereas SDW ones are enhanced when g_S is increased (this can be verified in the corresponding RG equations of Appendix B 2). Similarly, singlet SC instabilities are enhanced when g_s is increased, whereas triplet ones are enhanced when g_t is increased.

So, an increase of C_{back} implies an increase of the real space coupling g_1, and thus, from Eq. (A2), it favors CDW instabilities against SDW ones, and from Eq. (A1), it favors triplet SC instabilities and depresses singlet SC ones.

Similarly, an increase of C_{for} implies an increase of the real space coupling g_2, and thus, from Eq. (A2), it favors CDW and SDW instabilities, and from Eq. (A1), it depresses SC ones.

Of course, we examine here the influence of parameters C_{back} and C_{back} on the bare couplings. However, we believe that the flow could not just simply reverse this influence, even if the renormalized values of the couplings differ a lot from their bare values. Moreover, one verifies that these conclusions exactly correspond to the observed behavior.

The density wave interactions are on site, whereas the SC pairing are intersite (except for singlet s one), so we believe

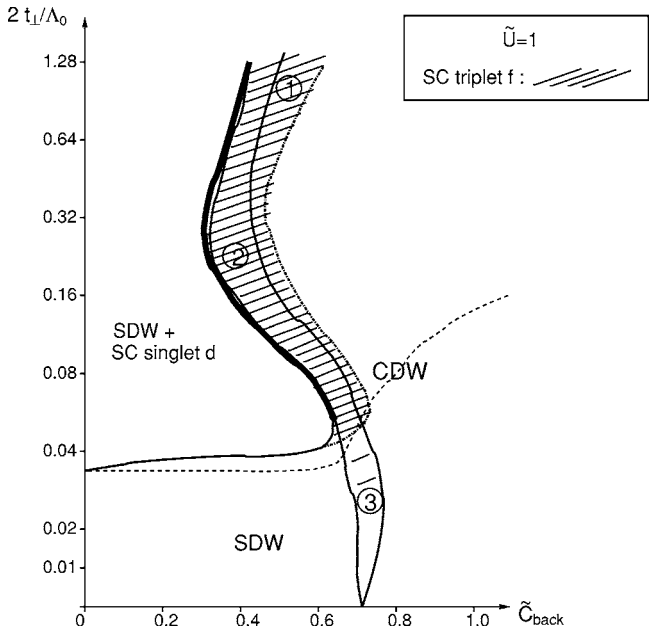

FIG. 16. Phase diagram for $\tilde{U}=1$. The shaded area indicates the divergence of the triplet susceptibility. The dashed line separates site or bond degenerated states (below) and nondegenerated ones (above). Other lines and domains are explained in the legend or in the text.

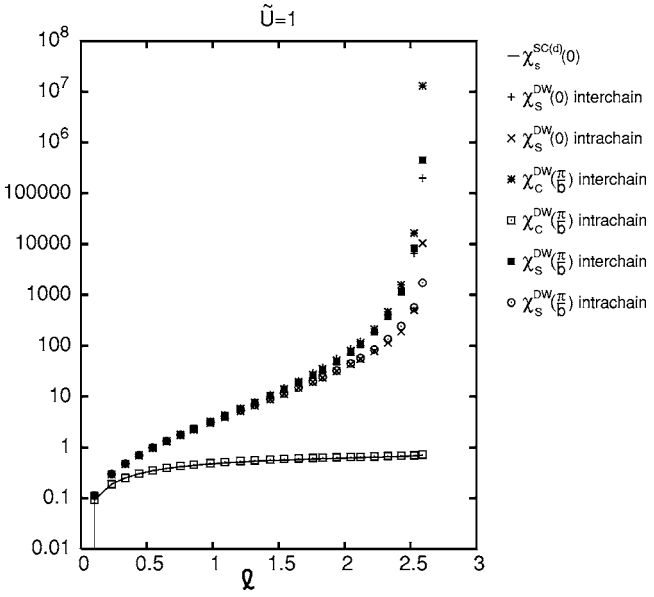

FIG. 17. Flow of the susceptibilities, $t_\perp=0.02$ and $\tilde{C}_{\text{for}}=0.95$.

that the DW instabilities appear first, and then enhance the SC ones. This is not true of the DW bond correlations, but we observed no divergences of these, and we have not studied any other sophisticated intersite DW excitation response.

From this point of view, the fact that π DW processes are favored, as we already discussed before, implies a π dephasing between both chains of the ladder. The π dephasing of the SDW thus fits perfectly singlet d condensate [which consists in a pairing of two electrons on a rung, with opposite spins, see Fig. 3(b)]. This accounts nicely for the appearance of singlet SC instability, induced by SDW one.

In the same trend of ideas, the π dephasing of the CDW fits triplet f_x condensate [which consists in a pairing of two electrons on each chain, one stepped by unity from the other, see Fig. 4(a)] and accounts for the appearance of triplet SC instability, induced by CDW one.

On the contrary, the triplet p_x condensate consists in two following electrons on one chain [see Fig. 4(b)], this pairing is not enhanced by CDW instabilities; in fact, it is the analog of singlet s condensate, which is not either enhanced by SDW instabilities, and is therefore disadvantaged, compared to d pairing.

As can be observed on Fig. 4, triplet f_x condensate are not incompatible with CDW. For instance, one could easily figure out a succession of condensate, with alternate spins, inducing back a global modulation of the chains. A similar scenario is not possible with triplet p condensate.

One should be aware that the symmetry classification we have used is very specific of the ladder system, and could not be extended to an infinite number of chains. The difference between p and f condensate is very subtle and the situation could reveal quite different in the general quasi-one-dimensional systems.

VII. CONCLUSION

We have investigated the phase diagram of a ladder system, in the Hubbard model, with an interchain coupling $t_\perp$, using functional RG method, in the OPI scheme. We have introduced an original parametrization of the $k_\parallel$ dependence, and obtained rather new results; in particular, we have proved the existence of a new phase with only SDW fluctuations, for small enough values of $t_\perp$. From the divergences of the scattering couplings, we induce that this phase is different from the one-dimensional solution. However, for very small values of $t_\perp$ ($t_\perp < \Lambda_0 10^{-4}$), we find the usual one-dimensional behavior.

Our results altogether prove that the $k_\parallel$ dependence is important and must be taken into account in such a ladder system. The fact that this variable became influential in a ladder does not mean that the corresponding couplings $g(2\Delta k_f, -2\Delta k_f, 0)$, etc., are relevant. In fact, if the cutoff $\Lambda \to 0$, these couplings are left out of the integrated band, so they could only be marginal.[28] However, the divergence takes place at Λ_c, which is of the order of Δk_f, and this explains why these couplings, which are shifted by $\pm 2\Delta k_f$ from the Fermi points, have a nontrivial behavior and have to be taken into account. Moreover, as already explained in Section IV B 1, during the flow, these couplings influence those, with all momenta at the Fermi points, until $\Lambda = 2\Delta k_f$. This influence is still sensitive, when the divergence takes place. This explains why we could distinguish a new phase, which has not yet been observed by usual methods.

When $t_\perp$ is very large, however (for instance, $t_\perp \sim \Lambda_0$), the flow continues up to $\Lambda_c \ll v_f \Delta k_f$ (otherwise, the integrated band would not vary much and the renormalized couplings neither differ much from their bare values), and the above argument applies, proving that couplings $g(2\Delta k_f, -2\Delta k_f, 0)$, etc., are marginal or irrelevant. In that case, $k_\parallel$ are not influential, and our results coincide indeed with former calculations.

We have also given a detailed classification of the response function, which provides a convenient tool for the determination of order parameters and of related susceptibilities, corresponding to different instability processes.

We are proceeding now to a complete study of the long range correlations, and in particular, of the uniform susceptibility. This task however proves quite difficult, because of the $k_\parallel$ dependence, which has to be carefully taken into account. We expect that the spin-gap will indeed disappear in the SDW phase we have brought to evidence.

We have also investigated the influence of interchain scattering, and showed that a backward interchain scattering can raise triplet superconductivity, a result consistent with the conclusions of a previous work by Bourbonnais *et al.*[29,30] on correlated quasi-one-dimensional metals. The appearance of triplet SC in a ladder is a very exciting and promising result, since various authors[40,41] claim to have found experimental evidence of these instabilities. Even the narrowness of the triplet SC existence region seems to fit the experimental data, which report high sensitivity of these fluctuations to some key parameters. This work gains to be compared with the previous work of Varma *et al.*, who did similar investigations.[42]

ACKNOWLEDGMENTS

We would like to thank N. Dupuis, S. Haddad, and B. Douçot for fruitful discussions and advice. J.C.N. wishes to

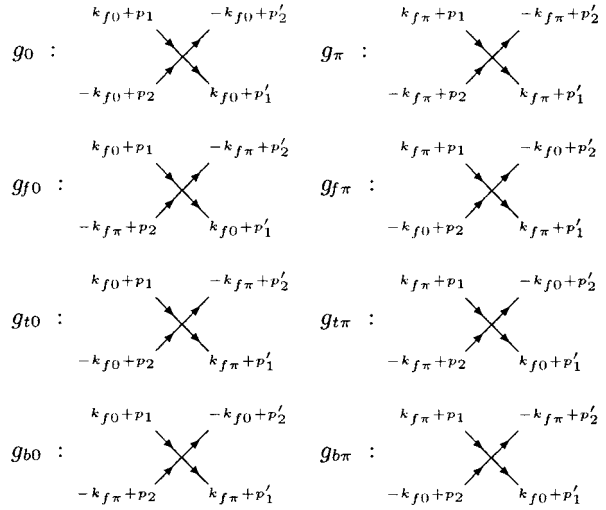

FIG. 18. Schematic definitions of the couplings g.

thank the Gottlieb Daimler- und Karl Benz-Stiftung for partial support.

APPENDIX A: COUPLINGS

1. Two-particle couplings

Here are the definitions of the different couplings g, from the two-particle parameter $\mathcal{G}$ (also see Fig. 18):

$$g_0(p_1,p_2,p_2',p_1') = \mathcal{G}(k_{f0}+p_1,-k_{f0}+p_2,-k_{f0}+p_2',k_{f0}+p_1'),$$

$$g_\pi(p_1,p_2,p_2',p_1') = \mathcal{G}(k_{f\pi}+p_1,-k_{f\pi}+p_2,-k_{f\pi}+p_2',k_{f\pi}+p_1'),$$

$$g_{f0}(p_1,p_2,p_2',p_1') = \mathcal{G}(k_{f0}+p_1,-k_{f\pi}+p_2,-k_{f\pi}+p_2',k_{f0}+p_1'),$$

$$g_{f\pi}(p_1,p_2,p_2',p_1') = \mathcal{G}(k_{f\pi}+p_1,-k_{f0}+p_2,-k_{f0}+p_2',k_{f\pi}+p_1'),$$

$$g_{t0}(p_1,p_2,p_2',p_1') = \mathcal{G}(k_{f0}+p_1,-k_{f0}+p_2,-k_{f\pi}+p_2',k_{f\pi}+p_1'),$$

$$g_{t\pi}(p_1,p_2,p_2',p_1') = \mathcal{G}(k_{f\pi}+p_1,-k_{f\pi}+p_2,-k_{f0}+p_2',k_{f0}+p_1'),$$

$$g_{b0}(p_1,p_2,p_2',p_1') = \mathcal{G}(k_{f0}+p_1,-k_{f\pi}+p_2,-k_{f0}+p_2',k_{f\pi}+p_1'),$$

$$g_{b\pi}(p_1,p_2,p_2',p_1') = \mathcal{G}(k_{f\pi}+p_1,-k_{f0}+p_2,-k_{f\pi}+p_2',k_{f0}+p_1').$$

The relations between the different representations can be found in Refs. 27 or 43. Here, they reduce to

$$g_s = -g_1 - g_2,$$

$$g_t = g_1 - g_2, \tag{A1}$$

$$g_C = g_2 - 2g_1,$$

$$g_S = g_2. \tag{A2}$$

2. Other couplings

Here are the definitions of the different couplings z, from the couplings to external fields $\mathcal{Z}$. (See also Fig. 19.)

$$z_0^{\mathrm{SC}}(p_1,p_2,q) =$$

$$\mathcal{Z}^{\mathrm{SC}}(-k_{f0}+p_1,k_{f0}+p_2,(q,0),0)$$

$$z_\pi^{\mathrm{SC}}(p_1,p_2,q) =$$

$$\mathcal{Z}^{\mathrm{SC}}(-k_{f\pi}+p_1,k_{f\pi}+p_2,(q,0),\pi)$$

$$z_+^{\mathrm{SC}}(p_1,p_2,q) =$$

$$\mathcal{Z}^{\mathrm{SC}}(-k_{f\pi}+p_1,k_{f0}+p_2,(q,\tfrac{\pi}{b}),0)$$

$$z_-^{\mathrm{SC}}(p_1,p_2,q) =$$

$$\mathcal{Z}^{\mathrm{SC}}(-k_{f0}+p_1,k_{f\pi}+p_2,(q,\tfrac{\pi}{b}),\pi)$$

$$z_0^{\mathrm{DW}}(p_1,p_2,q) =$$

$$\mathcal{Z}^{\mathrm{DW}}(-k_{f0}+p_1,k_{f0}+p_2,(q-2k_{f0},0),0)$$

$$z_\pi^{\mathrm{DW}}(p_1,p_2,q) =$$

$$\mathcal{Z}^{\mathrm{DW}}(-k_{f\pi}+p_1,k_{f\pi}+p_2,(q-2k_{f\pi},0),\pi)$$

$$z_+^{\mathrm{DW}}(p_1,p_2,q) =$$

$$\mathcal{Z}^{\mathrm{DW}}(-k_{f\pi}+p_1,k_{f0}+p_2,(q-k_{f0}-k_{f\pi},\tfrac{\pi}{b}),0)$$

$$z_-^{\mathrm{DW}}(p_1,p_2,q) =$$

$$\mathcal{Z}^{\mathrm{DW}}(-k_{f0}+p_1,k_{f\pi}+p_2,(q-k_{f0}-k_{f\pi},\tfrac{\pi}{b}),\pi)$$

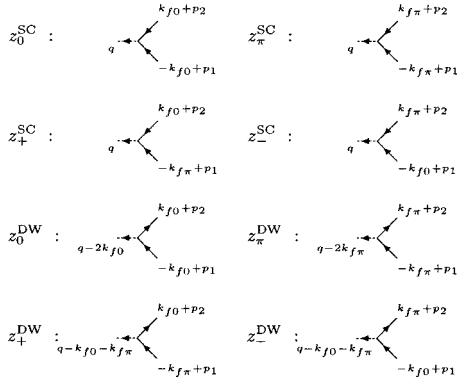

FIG. 19. Schematic definitions of the couplings z.

We omit the spin index α and the symmetry index Γ, and use the notation explained further in Appendix C 1. Remember that $\Gamma=s,d,g$ for $\alpha=s$ (singlet) and $\Gamma=p,f$ for $\alpha=t$ (triplet). The symmetry (s, $d_{x^2-y^2}$, g, p_x, f_x, or f_y) applying to each one is detailed in the main text:

$$z_0^{\mathrm{SC}}(p_1,p_2,q) = \mathcal{Z}^{\mathrm{SC}}(-k_{f0}+p_1,k_{f0}+p_2,(q,0),0),$$

$$z_\pi^{\mathrm{SC}}(p_1,p_2,q) = \mathcal{Z}^{\mathrm{SC}}(-k_{f\pi}+p_1,k_{f\pi}+p_2,(q,0),\pi),$$

$$z_+^{\mathrm{SC}}(p_1,p_2,q) = \mathcal{Z}^{\mathrm{SC}}\left(-k_{f\pi}+p_1,k_{f0}+p_2,\left(q,\frac{\pi}{b}\right),0\right),$$

$$z_-^{\mathrm{SC}}(p_1,p_2,q) = \mathcal{Z}^{\mathrm{SC}}\left(-k_{f0}+p_1,k_{f\pi}+p_2,\left(q,\frac{\pi}{b}\right),\pi\right),$$

$$z_0^{\mathrm{DW}}(p_1,p_2,q) = \mathcal{Z}^{\mathrm{DW}}(-k_{f0}+p_1,k_{f0}+p_2,(q-2k_{f0},0),0),$$

$$z_{\pi}^{\mathrm{DW}}(p_1,p_2,q) = \mathcal{Z}^{\mathrm{DW}}(-k_{f\pi}+p_1,k_{f\pi}+p_2,(q-2k_{f\pi},0),\pi),$$

$$z_{+}^{\mathrm{DW}}(p_1,p_2,q) = \mathcal{Z}^{\mathrm{DW}}\left(-k_{f\pi}+p_1,k_{f0}+p_2,\left(q-k_{f0}-k_{f\pi},\frac{\pi}{b}\right),0\right),$$

$$z_{-}^{\mathrm{DW}}(p_1,p_2,q) = \mathcal{Z}^{\mathrm{DW}}\left(-k_{f0}+p_1,k_{f\pi}+p_2,\left(q-k_{f0}-k_{f\pi},\frac{\pi}{b}\right),\pi\right).$$

APPENDIX B: RG EQUATIONS

We give here the detailed RG equations.

1. *g* couplings

Here are the RG equations for the couplings g, in (c,l,p) representation. The spin dependence is given, for all terms, by

$$\frac{dg_{\alpha}}{d\ell} = \sum_{\beta,\gamma} g_{\beta}(\mathcal{C}_{\alpha}^{\beta\gamma}+\mathcal{P}_{\alpha}^{\beta\gamma})g_{\gamma},$$

where $\mathcal{C}$ and $\mathcal{P}$ correspond, respectively, to the Cooper and Peierls channels, and are given, in the g-ology representation, by

$$\mathcal{C}_1 = -\begin{pmatrix}0 & 1\\ 1 & 0\end{pmatrix}, \quad \mathcal{C}_2 = -\begin{pmatrix}1 & 0\\ 0 & 1\end{pmatrix},$$

$$\mathcal{P}_1 = \begin{pmatrix}2 & -1\\ -1 & 0\end{pmatrix}, \quad \mathcal{P}_2 = \begin{pmatrix}0 & 0\\ 0 & -1\end{pmatrix},$$

see, for instance, Refs. 27, 43, and 44. In the following equations, all two first terms are Cooper ones, whereas all two last terms are Peierls ones; so, we omit the spin dependence, which is given by the above equations, for each term. One gets

$$\begin{aligned}\frac{d\tilde{g}_0}{d\ell}(c,l,p) = {}& \frac{\Lambda}{8\Lambda+4|c|}\Bigg[\sum_{\pm}\tilde{g}_0\left(c,\pm\left(\Lambda+\frac{|c|}{2}\right)+\frac{l+p}{2},\mp\left(\Lambda+\frac{|c|}{2}\right)+\frac{l+p}{2}\right)\tilde{g}_0\left(c,\mp\left(\Lambda+\frac{|c|}{2}\right)+\frac{l-p}{2},\mp\left(\Lambda+\frac{|c|}{2}\right)-\frac{l-p}{2}\right)\\ &+\sum_{\pm}\tilde{g}_{t0}\left(c,\pm\left(\Lambda+\frac{|c|}{2}\right)+\frac{l+p}{2},\mp\left(\Lambda+\frac{|c|}{2}\right)+\frac{l+p}{2}\right)\tilde{g}_{t\pi}\left(c,\mp\left(\Lambda+\frac{|c|}{2}\right)+\frac{l-p}{2},\mp\left(\Lambda+\frac{|c|}{2}\right)-\frac{l-p}{2}\right)\Bigg]\\ &+\frac{\Lambda}{8\Lambda+4|p|}\Bigg[\sum_{\pm}\tilde{g}_0\left(\mp\left(\Lambda+\frac{|p|}{2}\right)+\frac{c+l}{2},\pm\left(\Lambda+\frac{|p|}{2}\right)+\frac{c+l}{2},p\right)\tilde{g}_0\left(\mp\left(\Lambda+\frac{|p|}{2}\right)+\frac{c-l}{2},\mp\left(\Lambda+\frac{|p|}{2}\right)\right.\\ &\left.-\frac{c-l}{2},p\right)\Bigg]+\frac{\Lambda}{8\Lambda+4|p+2\Delta k_f|}\Bigg[\sum_{\pm}\tilde{g}_{b0}\left(\mp\left(\Lambda+\frac{|p+2\Delta k_f|}{2}\right)+\frac{c+l}{2}-\Delta k_f,\pm\left(\Lambda+\frac{|p+2\Delta k_f|}{2}\right)+\frac{c+l}{2}\right.\\ &\left.-\Delta k_f,p\right)\tilde{g}_{b\pi}\left(\mp\left(\Lambda+\frac{|p+2\Delta k_f|}{2}\right)+\frac{c-l}{2}+\Delta k_f,\mp\left(\Lambda+\frac{|p+2\Delta k_f|}{2}\right)-\frac{c-l}{2}+\Delta k_f,p+2\Delta k_f\right)\Bigg],\end{aligned}$$

$$\begin{aligned}\frac{d\tilde{g}_{f0}}{d\ell}(c,l,p) = {}& \frac{\Lambda}{8\Lambda+4|c|}\Bigg[\sum_{\pm}\tilde{g}_{f0}\left(c,\pm\left(\Lambda+\frac{|c|}{2}\right)+\frac{l+p}{2},\mp\left(\Lambda+\frac{|c|}{2}\right)+\frac{l+p}{2}\right)\tilde{g}_{f0}\left(c,\mp\left(\Lambda+\frac{|c|}{2}\right)+\frac{l-p}{2},\mp\left(\Lambda+\frac{|c|}{2}\right)\right.\\ &\left.-\frac{l-p}{2}\right)\Bigg]+\frac{\Lambda}{8\Lambda+4|c+2\Delta k_f|}\Bigg[\sum_{\pm}\tilde{g}_{b0}\left(c,\pm\left(\Lambda+\frac{|c+2\Delta k_f|}{2}\right)+\frac{l+p}{2}-\Delta k_f,\mp\left(c\Lambda+\frac{|c+2\Delta k_f|}{2}\right)+\frac{l+p}{2}\right.\\ &\left.-\Delta k_f\right)\tilde{g}_{b\pi}\left(c+2\Delta k_f,\mp\left(\Lambda+\frac{|c+2\Delta k_f|}{2}\right)+\frac{l-p}{2}+\Delta k_f,\mp\left(\Lambda+\frac{|c+2\Delta k_f|}{2}\right)-\frac{l-p}{2}+\Delta k_f\right)\Bigg]\\ &+\frac{\Lambda}{8\Lambda+4|p|}\Bigg[\sum_{\pm}\tilde{g}_{f0}\left(\mp\left(\Lambda+\frac{|p|}{2}\right)+\frac{c+l}{2},\pm\left(\Lambda+\frac{|p|}{2}\right)+\frac{c+l}{2},p\right)\tilde{g}_{f0}\left(\mp\left(\Lambda+\frac{|p|}{2}\right)+\frac{c-l}{2},\mp\left(\Lambda+\frac{|p|}{2}\right)\right.\\ &\left.-\frac{c-l}{2},p\right)+\sum_{\pm}\tilde{g}_{t0}\left(\mp\left(\Lambda+\frac{|p|}{2}\right)+\frac{c+l}{2},\pm\left(\Lambda+\frac{|p|}{2}\right)+\frac{c+l}{2},p\right)\tilde{g}_{t\pi}\left(\mp\left(\Lambda+\frac{|p|}{2}\right)+\frac{c-l}{2},\mp\left(\Lambda+\frac{|p|}{2}\right)\right.\\ &\left.-\frac{c-l}{2},p\right)\Bigg],\end{aligned}$$

$$\frac{d\tilde{g}_{t0}}{d\ell}(c,l,p)=\frac{\Lambda}{8\Lambda+4|c|}\Bigg[\sum_{\pm}\tilde{g}_0\Big(c,\pm\Big(\Lambda+\frac{|c|}{2}\Big)+\frac{l+p}{2},\mp\Big(\Lambda+\frac{|c|}{2}\Big)+\frac{l+p}{2}\Big)\tilde{g}_{t0}\Big(c,\mp\Big(\Lambda+\frac{|c|}{2}\Big)+\frac{l-p}{2},\mp\Big(\Lambda+\frac{|c|}{2}\Big)-\frac{l-p}{2}\Big)$$
$$+\sum_{\pm}\tilde{g}_{t0}\Big(c,\pm\Big(\Lambda+\frac{|c|}{2}\Big)+\frac{l+p}{2},\mp\Big(\Lambda+\frac{|c|}{2}\Big)+\frac{l+p}{2}\Big)\tilde{g}_{\pi}\Big(c,\mp\Big(\Lambda+\frac{|c|}{2}\Big)+\frac{l-p}{2},\mp\Big(\Lambda+\frac{|c|}{2}\Big)-\frac{l-p}{2}\Big)\Bigg]$$
$$+\frac{\Lambda}{8\Lambda+4|p|}\Bigg[\sum_{\pm}\tilde{g}_{t0}\Big(\mp\Big(\Lambda+\frac{|p|}{2}\Big)+\frac{c+l}{2},\pm\Big(\Lambda+\frac{|p|}{2}\Big)+\frac{c+l}{2},p\Big)\tilde{g}_{f\pi}\Big(\mp\Big(\Lambda+\frac{|p|}{2}\Big)+\frac{c-l}{2},\mp\Big(\Lambda+\frac{|p|}{2}\Big)$$
$$-\frac{c-l}{2},p\Big)+\sum_{\pm}\tilde{g}_{f0}\Big(\mp\Big(\Lambda+\frac{|p|}{2}\Big)+\frac{c+l}{2},\pm\Big(\Lambda+\frac{|p|}{2}\Big)+\frac{c+l}{2},p\Big)\tilde{g}_{t0}\Big(\mp\Big(\Lambda+\frac{|p|}{2}\Big)+\frac{c-l}{2},\mp\Big(\Lambda+\frac{|p|}{2}\Big)$$
$$-\frac{c-l}{2},p\Big)\Bigg],$$

$$\frac{d\tilde{g}_{b0}}{d\ell}(c,l,p)=\frac{\Lambda}{8\Lambda+4|c|}\Bigg[\sum_{\pm}\tilde{g}_{f0}\Big(c,\pm\Big(\Lambda+\frac{|c|}{2}\Big)+\frac{l+p}{2}+\Delta k_f,\mp\Big(\Lambda+\frac{|c|}{2}\Big)+\frac{l+p}{2}+\Delta k_f\Big)\tilde{g}_{b0}\Big(c,\mp\Big(\Lambda+\frac{|c|}{2}\Big)+\frac{l-p}{2}$$
$$-\Delta k_f,\mp\Big(\Lambda+\frac{|c|}{2}\Big)-\frac{l-p}{2}-\Delta k_f\Big)\Bigg]+\frac{\Lambda}{8\Lambda+4|c+2\Delta k_f|}\Bigg[\sum_{\pm}\tilde{g}_{b0}\Big(c,\pm\Big(\Lambda+\frac{|c+2\Delta k_f|}{2}\Big)+\frac{l+p}{2},\mp\Big(\Lambda$$
$$+\frac{|c+2\Delta k_f|}{2}\Big)+\frac{l+p}{2}\Big)\tilde{g}_{f\pi}\Big(c+2\Delta k_f,\mp\Big(\Lambda+\frac{|c+2\Delta k_f|}{2}\Big)\frac{l-p}{2},\mp\Big(\Lambda+\frac{|c+2\Delta k_f|}{2}\Big)-\frac{l-p}{2}\Big)\Bigg]$$
$$+\frac{\Lambda}{8\Lambda+4|p|}\Bigg[\sum_{\pm}\tilde{g}_0\Big(\mp\Big(\Lambda+\frac{|p|}{2}\Big)+\frac{c+l}{2}+\Delta k_f,\pm\Big(\Lambda+\frac{|p|}{2}\Big)+\frac{c+l}{2}+\Delta k_f,p\Big)\tilde{g}_{b0}\Big(\mp\Big(\Lambda+\frac{|p|}{2}\Big)+\frac{c-l}{2}$$
$$-\Delta k_f,\mp\Big(\Lambda+\frac{|p|}{2}\Big)-\frac{c-l}{2}-\Delta k_f,p\Big)\Bigg]+\frac{\Lambda}{8\Lambda+4|p+2\Delta k_f|}\Bigg[\sum_{\pm}\tilde{g}_{b0}\Big(\mp\Big(\Lambda+\frac{|p+2\Delta k_f|}{2}\Big)+\frac{c+l}{2},\pm\Big(\Lambda$$
$$+\frac{|p+2\Delta k_f|}{2}\Big)+\frac{c+l}{2},p\Big)\tilde{g}_{\pi}\Big(\mp\Big(\Lambda+\frac{|p+2\Delta k_f|}{2}\Big)+\frac{c-l}{2},\mp\Big(\Lambda+\frac{|p+2\Delta k_f|}{2}\Big)-\frac{c-l}{2},p+2\Delta k_f\Big)\Bigg].$$

2. z couplings

Here are the RG equations for the couplings z, in (k,c,p) representation. The z^{SC} couplings should be written in the singlet or triplet representation ($\alpha=s,t$), and the z^{DW} couplings should be written in the charge/spin representation ($\alpha=C,S$). Then, the spin dependence simply writes, for each one

$$\frac{dz_\alpha}{d\ell}=g_\alpha z_\alpha$$

and will therefore be again omitted. One gets

$$\frac{dz_0^{\mathrm{SC}}}{d\ell}(c,k)=\frac{\Lambda}{4\Lambda+2|c|}\Bigg[\sum_{\pm}\tilde{g}_0\Big(c,\pm\Big(\Lambda+\frac{|c|}{2}\Big)+\frac{c}{2}-k,$$
$$\mp\Big(\Lambda+\frac{|c|}{2}\Big)+\frac{c}{2}-k\Big)z_0^{\mathrm{SC}}\Big(c,\pm\Big(\Lambda+\frac{|c|}{2}\Big)+\frac{c}{2}\Big)$$
$$+\sum_{\pm}\tilde{g}_{t0}\Big(c,\pm\Big(\Lambda+\frac{|c|}{2}\Big)+\frac{c}{2}-k,\mp\Big(\Lambda+\frac{|c|}{2}\Big)$$
$$+\frac{c}{2}-k\Big)z_\pi^{\mathrm{SC}}\Big(c,\pm\Big(\Lambda+\frac{|c|}{2}\Big)+\frac{c}{2}\Big)\Bigg],$$

$$\frac{dz_+^{\mathrm{SC}}}{d\ell}(c,k)=\frac{\Lambda}{4\Lambda+2|c|}\sum_{\pm}\tilde{g}_{f0}\Big(c,\pm\Big(\Lambda+\frac{|c|}{2}\Big)+\frac{c}{2}-k,$$
$$\mp\Big(\Lambda+\frac{|c|}{2}\Big)+\frac{c}{2}-k\Big)z_+^{\mathrm{SC}}\Big(c,\pm\Big(\Lambda+\frac{|c|}{2}\Big)+\frac{c}{2}\Big)$$
$$+\frac{\Lambda}{4\Lambda+2|c+2\Delta k_f|}\sum_{\pm}\tilde{g}_{b0}\Big(c,\pm\Big(\Lambda+\frac{|c+2\Delta k_f|}{2}\Big)$$
$$+\frac{c}{2}-\Delta k_f-k,\mp\Big(\Lambda+\frac{|c+2\Delta k_f|}{2}\Big)$$
$$+\frac{c}{2}-\Delta k_f-k\Big)z_-^{\mathrm{SC}}\Big(c+2\Delta k_f,\pm\Big(\Lambda+\frac{|c+2\Delta k_f|}{2}\Big)$$
$$+\frac{c}{2}+\Delta k_f\Big),$$

$$\frac{dz_0^{\mathrm{DW}}}{d\ell}(p,k) = \frac{\Lambda}{4\Lambda+2|p|}\sum_{\pm}\tilde{g}_0\left(\pm\left(\Lambda+\frac{|p|}{2}\right)+\frac{p}{2}+k,\right.$$
$$\left.\pm\left(\Lambda+\frac{|p|}{2}\right)-\frac{p}{2}-k,p\right)z_0^{\mathrm{DW}}\left(p,\pm\left(\Lambda+\frac{|p|}{2}\right)\right.$$
$$\left.-\frac{p}{2}\right)+\frac{\Lambda}{4\Lambda+2|p+2\Delta k_f|}\sum_{\pm}\tilde{g}_{b\pi}\left(\pm\left(\Lambda\right.\right.$$
$$\left.+\frac{|p+2\Delta k_f|}{2}\right)+\frac{p}{2}+\Delta k_f+k,\pm\left(\Lambda\right.$$
$$\left.+\frac{|p+2\Delta k_f|}{2}\right)$$
$$\left.-\frac{p}{2}+\Delta k_f-k,p+2\Delta k_f\right)z_\pi^{\mathrm{DW}}\left(p+2\Delta k_f,\right.$$
$$\left.\pm\left(\Lambda+\frac{|p+2\Delta k_f|}{2}\right)-\frac{p}{2}-\Delta k_f\right),$$

$$\frac{dz_+^{\mathrm{DW}}}{d\ell}(p,k) = \frac{\Lambda}{4\Lambda+2|p|}\left[\sum_{\pm}\tilde{g}_{f0}\left(\pm\left(\Lambda+\frac{|p|}{2}\right)+\frac{p}{2}+k,\right.\right.$$
$$\left.\pm\left(\Lambda+\frac{|p|}{2}\right)-\frac{p}{2}-k,p\right)z_+^{\mathrm{DW}}\left(p,\pm\left(\Lambda+\frac{|p|}{2}\right)\right.$$
$$\left.-\frac{p}{2}\right)+\sum_{\pm}\tilde{g}_{t\pi}\left(\pm\left(\Lambda+\frac{|p|}{2}\right)\right.$$
$$\left.+\frac{p}{2}+k,\pm\left(\Lambda+\frac{|p|}{2}\right)\right.$$
$$\left.\left.-\frac{p}{2}-k,p\right)z_-^{\mathrm{DW}}\left(p,\pm\left(\Lambda+\frac{|p|}{2}\right)-\frac{p}{2}\right)\right].$$

3. χ couplings

Here are the RG equations for the susceptibilities χ, with the same spin dependence as the corresponding z couplings, which is again omitted,

$$\frac{d\chi_0^{\mathrm{SC}}}{d\ell}(q) = -\frac{\Lambda}{4\Lambda+2|q|}\left[\sum_{\pm}z_0^{\mathrm{SC}}\left(q,\pm\left(\Lambda+\frac{|q|}{2}\right)+\frac{q}{2}\right)^2\right.$$
$$\left.+\sum_{\pm}z_\pi^{\mathrm{SC}}\left(q,\pm\left(\Lambda+\frac{|q|}{2}\right)+\frac{q}{2}\right)^2\right],$$

$$\frac{d\chi_+^{\mathrm{SC}}}{d\ell}(q) = -\frac{\Lambda}{4\Lambda+2|q|}\sum_{\pm}z_+^{\mathrm{SC}}\left(q,\pm\left(\Lambda+\frac{|q|}{2}\right)+\frac{q}{2}\right)^2$$
$$-\frac{\Lambda}{4\Lambda+2|q+2\Delta k_f|}\sum_{\pm}z_-^{\mathrm{SC}}\left(q+2\Delta k_f,\pm\left(\Lambda\right.\right.$$
$$\left.\left.+\frac{|q+2\Delta k_f|}{2}\right)+\frac{q}{2}+\Delta k_f\right)^2,$$

$$\frac{d\chi_0^{\mathrm{DW}}}{d\ell}(q) = -\frac{\Lambda}{4\Lambda+2|q|}\sum_{\pm}z_0^{\mathrm{DW}}\left(-q,\pm\left(\Lambda+\frac{|q|}{2}\right)+\frac{q}{2}\right)^2$$
$$-\frac{\Lambda}{4\Lambda+2|q-2\Delta k_f|}\sum_{\pm}z_\pi^{\mathrm{DW}}\left(-q+2\Delta k_f,\pm\left(\Lambda\right.\right.$$
$$\left.\left.+\frac{|q-2\Delta k_f|}{2}\right)+\frac{q}{2}-\Delta k_f\right)^2,$$

$$\frac{d\chi_+^{\mathrm{DW}}}{d\ell}(q) = -\frac{\Lambda}{4\Lambda+2|q|}\left[\sum_{\pm}z_+^{\mathrm{DW}}\left(-q,\pm\left(\Lambda+\frac{|q|}{2}\right)+\frac{q}{2}\right)^2\right.$$
$$\left.+\sum_{\pm}z_-^{\mathrm{DW}}\left(-q,\pm\left(\Lambda+\frac{|q|}{2}\right)+\frac{q}{2}\right)^2\right).$$

APPENDIX C: SYMMETRIES

1. Ordinary symmetries

If we apply the conjugation symmetry C to the two-particle coupling $\mathcal{G}$, we get

$$\mathcal{G}(P_1',P_2',P_2,P_1) = \mathcal{G}(-P_1,-P_2,-P_2',-P_1').$$

If we apply A, we get

$$\mathcal{G}_C(P_2,P_1,P_2',P_1') = -2\mathcal{G}_C(P_1,P_2,P_2',P_1') - 3\mathcal{G}_S(P_1,P_2,P_2',P_1'),$$

$$\mathcal{G}_S(P_2,P_1,P_2',P_1') = \mathcal{G}_C(P_1,P_2,P_2',P_1') + 2\mathcal{G}_S(P_1,P_2,P_2',P_1').$$

If we apply A', we get

$$\mathcal{G}_C(P_1,P_2,P_1',P_2') = -2\mathcal{G}_C(P_1,P_2,P_2',P_1') - 3\mathcal{G}_S(P_1,P_2,P_2',P_1'),$$

$$\mathcal{G}_S(P_1,P_2,P_1',P_2') = \mathcal{G}_C(P_1,P_2,P_2',P_1') + 2\mathcal{G}_S(P_1,P_2,P_2',P_1').$$

Finally, from parity P conservation, we get

$$\mathcal{G}(P_1,P_2,P_2',P_1') = \mathcal{G}(-P_1,-P_2,-P_2',-P_1').$$

Note that AA' simply gives $\mathcal{G}(P_2,P_1,P_1',P_2') = \mathcal{G}(P_1,P_2,P_2',P_1')$.

For the SC instability coupling, we will write the two-dimensional interaction vector $\mathbf{Q}=(Q_\parallel,Q_\perp)$, and add a discrete variable $\theta=0,\pi$, which indicates whether the R particle is on the 0 band ($\theta=0$) or the π band ($\theta=\pi$); this way, one can distinguish 0-0, 0-π, π-0 or π-π processes (use Fig. 2 for help).

If we apply P, we get

$$\mathcal{Z}^{\mathrm{SC}}(-P_1,-P_2,(-Q_\parallel,Q_\perp),\theta) = \mathcal{Z}^{\mathrm{SC}}(P_1,P_2,(Q_\parallel,Q_\perp),\theta).$$

If we apply A or A' (note that in H_{SC}, the term with incoming momenta P_1 and P_2 is conjugate to that with outgoing momenta P_1 and P_2), we get

$$\mathcal{Z}_\alpha^{\mathrm{SC}}(P_2,P_1,(Q_\parallel,0),\theta) = \mathcal{Z}_\alpha^{\mathrm{SC}}(P_1,P_2,(Q_\parallel,0),\theta), \quad \alpha=s,t,$$

$$\mathcal{Z}_s^{\mathrm{SC}(s)}\left(P_2,P_1,\left(Q_\parallel,\frac{\pi}{b}-Q_\perp\right),\theta\right) = \mathcal{Z}_s^{\mathrm{SC}(s)}(P_1,P_2,(Q_\parallel,Q_\perp),\pi-\theta),$$

$$\mathcal{Z}_s^{\mathrm{SC}(g)}\left(P_2,P_1,\left(Q_\parallel,\frac{\pi}{b}-Q_\perp\right),\theta\right) = -\mathcal{Z}_s^{\mathrm{SC}(g)}(P_1,P_2,(Q_\parallel,Q_\perp),\pi-\theta),$$

$$\mathcal{Z}_t^{\mathrm{SC}(p_x)}\left(P_2,P_1,\left(Q_\parallel,\frac{\pi}{b}-Q_\perp\right),\theta\right) = \mathcal{Z}_t^{\mathrm{SC}(p_x)}(P_1,P_2,(Q_\parallel,Q_\perp),\pi-\theta),$$

$$\mathcal{Z}_t^{\mathrm{SC}(f_y)}\left(P_2,P_1,\left(Q_\parallel,\frac{\pi}{b}-Q_\perp\right),\theta\right) = -\mathcal{Z}_t^{\mathrm{SC}(f_y)}(P_1,P_2,(Q_\parallel,Q_\perp),\pi-\theta).$$

Finally, it is interesting to note that $\mathcal{Z}_s^{\mathrm{SC}}$ (singlet) and $\mathcal{Z}_{t_x}^{\mathrm{SC}}$ (triplet) change sign under S and are invariant under C, while $\mathcal{Z}_{t_y}^{\mathrm{SC}}$ and $\mathcal{Z}_{t_z}^{\mathrm{SC}}$ (both triplet) do the opposite.

For the DW instability coupling, we use the same notation. Note that $Q_\parallel$ writes $-(p_1-p_2+2k_{f\theta})$ for intraband processes, and $-(p_1-p_2+k_{f0}+k_{f\pi})$ for interband ones. If we apply CS, we get

$$\mathcal{Z}^{\mathrm{DW}}(-P_1,-P_2,(2k_{f\theta}-Q_\parallel,Q_\perp),\theta) = \mathcal{Z}^{\mathrm{DW}}(P_1,P_2,(-2k_{f\theta}+Q_\parallel,Q_\perp),\theta),$$

and if we apply AS, we get

$$\mathcal{Z}^{\mathrm{DW}}(P_2,P_1,(2k_{f\theta}-Q_\parallel,Q_\perp),\theta) = \pm\,\mathcal{Z}^{\mathrm{DW}}(P_1,P_2,(-2k_{f\theta}+Q_\parallel,Q_\perp),\theta),$$

$$\mathcal{Z}^{\mathrm{DW}}\left(P_2,P_1,\left(k_{f0}+k_{f\pi}-Q_\parallel,\frac{\pi}{b}-Q_\perp\right),\theta\right) = \mp\,\mathcal{Z}^{\mathrm{DW}}(P_1,P_2,(-k_{f0}-k_{f\pi}+Q_\parallel,Q_\perp),\pi-\theta),$$

where $\pm$ reads $+$ for site ordering, and $-$ for bond ordering.

2. Supplementary symmetry

When we apply the special symmetry $\tilde{C}$ to two-particle couplings $\mathcal{G}$, we get

$$\mathcal{G}(k_{f0}+k_{f\pi}-P_1,k_{f0}+k_{f\pi}-P_2,k_{f0}+k_{f\pi}-P_2',k_{f0}+k_{f\pi}-P_1') = \mathcal{G}(P_1,P_2,P_2',P_1').$$

When we apply the special symmetry $\tilde{C}$ to SC instabilities $\mathcal{Z}_{\mathrm{SC}}$, we get

$$\mathcal{Z}_\alpha^{\mathrm{SC}(\Gamma)}(-k_{f0}-k_{f\pi}-P_1,k_{f0}+k_{f\pi}-P_2,(-Q_\parallel,0),\theta) = \pm\,\mathcal{Z}_\alpha^{\mathrm{SC}(\Gamma)}(P_1,P_2,(Q_\parallel,0),\pi-\theta),$$

$$\mathcal{Z}_\alpha^{\mathrm{SC}(\Gamma)}\left(-k_{f0}-k_{f\pi}-P_1,k_{f0}+k_{f\pi}-P_2,\left(-Q_\parallel,\frac{\pi}{b}-Q_\perp\right),\theta\right) = \pm\,\mathcal{Z}_\alpha^{\mathrm{SC}(\Gamma)}(P_1,P_2,(Q_\parallel,Q_\perp),\pi-\theta),$$

where $\pm$ reads $+$ for $\alpha=s$, $\Gamma=s$ or for $\alpha=t$, $\Gamma=p_x$, and $-$ for $\alpha=s$, $\Gamma=d,g$ or for $\alpha=t$, $\Gamma=f_x,f_y$.

When we apply the special symmetry $\tilde{C}$ to DW instabilities $\mathcal{Z}_{\mathrm{DW}}$, we get

$$\mathcal{Z}^{\mathrm{DW}}(-k_{f0}-k_{f\pi}-P_1,k_{f0}+k_{f\pi}-P_2,(2k_{f\theta}-Q_\parallel,0),\theta) = \pm\,\mathcal{Z}^{\mathrm{DW}}(P_1,P_2,(-2k_{f[\pi-\theta]}+Q_\parallel,0),\pi-\theta),$$

$$\mathcal{Z}^{\mathrm{DW}}\left(-k_{f0}-k_{f\pi}-P_1,k_{f0}+k_{f\pi}-P_2,\left(-k_{f0}-k_{f\pi}-Q_\parallel,\frac{\pi}{b}-Q_\perp\right),\theta\right) = \pm\,\mathcal{Z}^{\mathrm{DW}}(P_1,P_2,(-k_{f0}-k_{f\pi}+Q_\parallel,Q_\perp),\pi-\theta),$$

where $\pm$ reads $+$ for site ordering, and $-$ for bond ordering.

3. g_b orbits

Here are the 8 first orbits of the g_{b0} coefficient, in (c,l,p) representation:

$\{(0,0,-2\Delta k_f,0),(0,-2\Delta k_f,0),(-2\Delta k_f,0,0),$
$(-2\Delta k_f,-2\Delta k_f,-2\Delta k_f)\}$ are sym. equiv.,

$\{(-4\Delta k_f,-4\Delta k_f,-2\Delta k_f),(-4\Delta k_f,2\Delta k_f,0),$
$(2\Delta k_f,-4\Delta k_f,0),$
$(2\Delta k_f,2\Delta k_f,-2\Delta k_f)\}$ id.,

$\{(0,-4\Delta k_f,2\Delta k_f),(0,2\Delta k_f,-4\Delta k_f),(-2\Delta k_f,-4\Delta k_f,-4\Delta k_f),$
$(-2\Delta k_f,2\Delta k_f,2\Delta k_f)\}$ id.,

$\{(-4\Delta k_f,0,2\Delta k_f),(-4\Delta k_f,-2\Delta k_f,-4\Delta k_f),(2\Delta k_f,0,-4\Delta k_f),$
$(2\Delta k_f,-2\Delta k_f,2\Delta k_f)\}$ id.,

$\{(0,-4\Delta k_f,-2\Delta k_f),(0,2\Delta k_f,0),(-2\Delta k_f,-4\Delta k_f,0),$
$(-2\Delta k_f,2\Delta k_f,-2\Delta k_f)\}$ id.,

$\{(-4\Delta k_f,0,-2\Delta k_f),(-4\Delta k_f,-2\Delta k_f,0),(2\Delta k_f,0,0),$
$(2\Delta k_f,-2\Delta k_f,-2\Delta k_f)\}$ id.,

$\{(0,0,2\Delta k_f),(0,-2\Delta k_f,-4\Delta k_f),$
$(-2\Delta k_f,0,-4\Delta k_f),(-2\Delta k_f,-2\Delta k_f,2\Delta k_f)\}$ id.,

$\{(-4\Delta k_f,-4\Delta k_f,2\Delta k_f),(-4\Delta k_f,2\Delta k_f,-4\Delta k_f),$
$(2\Delta k_f,-4\Delta k_f,-4\Delta k_f),(2\Delta k_f,2\Delta k_f,2\Delta k_f)\}$ id.

APPENDIX D: FOURIER TRANSFORM

Creation and annihilation operators. If one writes $\psi_{ij\sigma}^\dagger$ the creator of a particle of spin σ, located in real space at posi-

tion i ($i \in \{1,\ldots,N\}$), on chain j ($j=\pm 1$), the representation in the momentum space writes

$$L_{p,0,\sigma} = \Psi_{(-k_{f0}+p,0)\sigma} = \sum_{ij} \psi_{ij\sigma} e^{-\mathrm{i}(p-k_{f0})ia},$$

$$L_{p,\pi,\sigma} = \Psi_{(-k_{f\pi}+p,\pi/b)\sigma} = \sum_{ij} j\psi_{ij\sigma} e^{-\mathrm{i}(p-k_{f\pi})ia},$$

$$R_{p,0,\sigma} = \Psi_{(k_{f0}+p,0)\sigma} = \sum_{ij} \psi_{ij\sigma} e^{-\mathrm{i}(p+k_{f0})ia},$$

$$R_{p,\pi,\sigma} = \Psi_{(k_{f\pi}+p,\pi/b)\sigma} = \sum_{ij} j\psi_{ij\sigma} e^{-\mathrm{i}(p+k_{f\pi})ia},$$

with the notations of the text. $\Psi_{\mathbf{k}\sigma}$ stands for the absolute momentum representation, while L and R stand for the relative momentum representation. These relations are given for annihilation operators; one must take the complex conjugation to obtain those for the creation operators.

The reverse relations simply write, in terms of the Ψ operators,

$$\psi_{ij\sigma} = \int_{-\pi/a}^{\pi/a} \frac{adP}{4\pi} e^{\mathrm{i}aip} (\Psi_{(P,0),\sigma} + j\Psi_{(P,\pi/b),\sigma}),$$

but one can also express them in terms of the L and R operators. Then, one can check that this transformation is the inverse of the first one.

Electron-electron pair operator. In real space, the SC order parameters are the mean value of the electron-electron pair operator, which writes

$$O^{\alpha}(\mathbf{X}) = \sum_{\substack{\mathbf{X}' \\ \sigma\sigma'}} \psi_{\mathbf{X}\sigma}\psi_{\mathbf{X}'\sigma'}\Gamma(\mathbf{X},\mathbf{X}')\tau^{\alpha}_{\sigma\sigma'}.$$

To each $\mathbf{Q}=(Q_{\parallel},Q_{\perp})$ corresponds a Fourier component

$$O^{\alpha}(\mathbf{Q}) = \sum_{\mathbf{X}} e^{-\mathbf{Q}\cdot\mathbf{X}} O^{\alpha}(\mathbf{X}) = \sum_{ij} e^{-\mathrm{i}(aQ_{\parallel}i+bQ_{\perp}j/2)} O^{\alpha}(\mathbf{X}).$$

We only keep the components $\mathbf{Q}$ which lead to singularities; as explained in the main text, they are (0,0) and $(\pm\Delta k_f, \pi/b)$. So, using the short notation 0 for the first and $\pi_{\pm}$ for the second, one gets

$$O^{\alpha}(0) = \sum_i O^{\alpha}(ai,1) + O^{\alpha}(ai,-1)$$

and

$$O^{\alpha}(\pi_{\pm}) = \sum_i -\mathrm{i}e^{\mp \mathrm{i}\Delta k_f a}(O^{\alpha}(ai,1) - O^{\alpha}(ai,-1)),$$

where the main factor $O^{\alpha}(ai,1)\pm O^{\alpha}(ai,-1) = \sum_{\substack{jj' \\ \sigma\sigma'}} (\pm 1)^j \psi_{ij\sigma}\phi_{i'j'\sigma'}\Gamma(a(i-i'),b(j-j')/2)\tau^{\alpha}_{\sigma\sigma'}$ is the mixed representation of the pair operator.[45]

Eventually, the $\psi_{ij\sigma}$ can be expressed in terms of the $\Psi_{\mathbf{P}\sigma}$, so that the components write

$$O^{\alpha}(\mathbf{Q}) = \int_{-\pi/a}^{\pi/a} \frac{adP}{4\pi} \sum_{\theta=0,\pi} z_{\mathbf{Q}}(\mathbf{p}) \sum_{\sigma\sigma'} \Psi_{\mathbf{p},\sigma}\Psi_{\mathbf{Q}-\mathbf{p},\sigma'}\tau^{\alpha}_{\sigma\sigma'},$$

where $\mathbf{p}=(P,\theta/b)$ and we will also use $\mathbf{Q}=(Q_{\parallel},Q_{\perp})$. Be careful that, for instance, with $\mathbf{Q}=(\Delta k_f,\pi/b)$ and $\mathbf{p}=(p-k_{f0},0)$, and thus $\Psi_{\mathbf{p},\sigma}=L_{p,0\sigma}$, the calculation of $\Psi_{\mathbf{Q}-\mathbf{p},\sigma'}$ is not immediate; one gets $\Psi_{\mathbf{Q}-\mathbf{p},\sigma'} = \Psi_{(\Delta k_f - p + k_{f0},\pi/b),\sigma'} = R_{2\Delta k_f - p,\pi,\sigma'}$.

With $\Gamma(\mathbf{X},\mathbf{X}') = \delta_{ii'}\delta_{jj'}$, one finds $z_0(\mathbf{p})=1$ (singlet 0 condensate of s symmetry), and $z_{\pi_{\pm}}(\mathbf{p}) = -\mathrm{i}$ (singlet π condensate of s symmetry). With $\Gamma(\mathbf{X},\mathbf{X}') = \delta_{ii'}\delta_{j,-j'}$, one finds $z_0(\mathbf{p}) = \cos(\theta)$ (singlet 0 condensate of d symmetry) and $z_{\pi_{\pm}}(\mathbf{p}) = \mathrm{i}\cos(\theta)$ (triplet π condensate of f_y symmetry). With $\Gamma(\mathbf{X},\mathbf{X}') = \delta_{i,i'\mp 1}\delta_{j,-j'}$, one finds $z_0(\mathbf{p}) = \cos(aP)\cos(\theta)$ (singlet 0 condensate of extended d symmetry), as well as $z_0(\mathbf{p}) = -\mathrm{i}\sin(aP)\cos(\theta)$ (triplet 0 condensate of f_x symmetry), and $z_{\pi_{\pm}}(\mathbf{p}) = \sin(a(P \mp \Delta k_f/2))\cos(\theta)$ (singlet π condensate of g symmetry) or $z_{\pi_{\pm}}(\mathbf{p}) = \mathrm{i}e^{\pm \mathrm{i}(\Delta k_f a/2)}\cos(a(P \mp \Delta k_f/2))\cos(\theta)$ (triplet π condensate of extended f_y symmetry). With $\Gamma(\mathbf{X},\mathbf{X}') = \delta_{i,i'\mp 1}\delta_{jj'}$, one finds $z_0(\mathbf{p}) = \cos(aP)$ (singlet 0 condensate of extended s symmetry) or $z_0(\mathbf{p}) = -\mathrm{i}\sin(aP)$ (triplet 0-condensate of p_x symmetry), and $z_{\pi_{\pm}}(\mathbf{p}) = -\mathrm{i}e^{\pm \mathrm{i}(\Delta k_f a/2)}\cos(a(P \mp \Delta k_f/2))$ (singlet π condensate of extended s symmetry) or $z_{\pi_{\pm}}(\mathbf{p}) = -e^{\pm \mathrm{i}(\Delta k_f a/2)}\sin(a(P \mp \Delta k_f/2))$ (triplet π condensate of p_x symmetry).

Electron-hole pair operator. It is almost the same, with the product of a creation and an annihilation operators; be careful, however, that, in reciprocal space, one gets

$$\sum_{\sigma\sigma'} \int_{-\pi/a}^{\pi/a} \frac{adP}{4\pi} \Psi^{\dagger}_{\mathbf{p}\sigma}\Psi_{\mathbf{Q}+\mathbf{p}\sigma'} z(\mathbf{p}) \tau^{\alpha}_{\sigma\sigma'}.$$

[1] M. Azuma, Z. Hiroi, M. Takano, K. Ishida, and Y. Kitaoka, Phys. Rev. Lett. **73**, 3463 (1994).

[2] E. M. McCarron, Mater. Res. Bull. **23**, 1355 (1988); M. Sigrist, *ibid.* **23**, 1429 (1988).

[3] Z. Hiroi and M. Takano, Nature (London) **377**, 41 (1995).

[4] For a review of experimental results, see E. Dagotto, Rep. Prog. Phys. **62**, 1525 (1999).

[5] K. Penc and J. Sólyom, Phys. Rev. B **41**, 704 (1990).

[6] T. Giamarchi and H. J. Schulz, J. Phys. (France) **49**, 819 (1988).

[7] M. Tsuchiizu, P. Donohue, Y. Suzumura, and T. Giamarchi, Eur. Phys. J. B **19**, 185 (2001).

[8] J. I. Kishine and K. Yonemitsu, J. Phys. Soc. Jpn. **67**, 1714 (1998).

[9] K. Le Hur, Phys. Rev. B **63**, 165110 (2001).

[10] S. Haddad, S. Charfi-Kaddour, M. Heritier, and R. Bennaceur, J. Phys. IV **10**, 3 (2000).

[11] E. Dagotto, J. Riera, and D. Scalapino, Phys. Rev. B **45**, 5744 (1992).

[12] M. Fabrizio, Phys. Rev. B **48**, 15838 (1993).
[13] D. V. Khveshchenko and T. M. Rice, Phys. Rev. B **50**, 252 (1993).
[14] T. Barnes, E. Dagotto, J. Riera, and E. S. Swanson, Phys. Rev. B **47**, 3196 (1993).
[15] H.-H. Lin, L. Balents, and M. P. A. Fisher, Phys. Rev. B **56**, 6569 (1997).
[16] A. M. Finkel'stein and A. I. Larkin, Phys. Rev. B **47**, 10461 (1993).
[17] H. J. Schulz, Phys. Rev. B **53**, R2959 (1996).
[18] E. Orignac and T. Giamarchi, Phys. Rev. B **56**, 7167 (1997).
[19] K. Kuroki and H. Aoki, Phys. Rev. Lett. **72**, 2947 (1994).
[20] D. V. Khveshchenko, Phys. Rev. B **50**, 380 (1993).
[21] D. J. Scalapino, J. Low Temp. Phys. **117**, 179 (1999).
[22] R. M. Noack, S. R. White, and D. J. Scalapino, Phys. Rev. Lett. **73**, 882 (1994).
[23] J. I. Kishine and K. Yonemitsu, J. Phys. Soc. Jpn. **67**, 2590 (1998).
[24] Y. Park, S. Liang, and T. K. Lee, Phys. Rev. B **59**, 2587 (1999).
[25] W. Metzner, C. Castellani, and C. Di Castro, Adv. Phys. **47**, 317 (1998).
[26] C. Honerkamp, Ph.D. thesis, Naturwissenschaften ETH Zürich, Nr. 13868, 2000.
[27] C. Halboth, Ph.D. thesis, RWTH Aachen, 1999.
[28] R. Shankar, Rev. Mod. Phys. **66**, 129 (1994).
[29] C. Bourbonnais and R. Duprat, Bull. Am. Phys. Soc. **49**, 179 (2004).
[30] J. C. Nickel, R. Duprat, C. Bourbonnais, and N. Dupuis, cond-mat/0502614.
[31] S. Dusuel, F. V. de Abreu, and B. Douçot, Phys. Rev. B **65**, 094505 (2002).
[32] J. Sólyom, Adv. Phys. **28**, 201 (1979).
[33] C. Honerkamp, M. Salmhofer, N. Furukawa, and T. M. Rice, Phys. Rev. B **63**, 035109 (2001).
[34] B. Binz, D. Baeriswyl, and B. Douçot, Ann. Phys. (N.Y.) **12**, 704 (2003).
[35] C. Bourbonnais, in *Strongly Interacting Fermions and High-T_c Superconductivity*, edited by B. Douçot and J. Zinn-Justin, Les Houches LVI, 1991 (Elsevier Science, Amsterdam, 1995).
[36] V. N. Prigodin and Y. A. Firsov, Sov. Phys. JETP **49**, 813 (1979).
[37] P. A. Lee, T. M. Rice, and R. A. Klemm, Phys. Rev. B **15**, 2984 (1977).
[38] V. J. Emery, Synth. Met. **13**, 21 (1986).
[39] N. Furukawa, T. M. Rice, and M. Salmhofer, Phys. Rev. Lett. **81**, 3195 (1998).
[40] I. J. Lee, P. M. Chaikin, and M. J. Naughton, Phys. Rev. B **62**, R14669 (2000); I. J. Lee, S. E. Brown, W. G. Clark, M. J. Strouse, M. J. Naughton, W. Kang, and P. M. Chaikin, Phys. Rev. Lett. **88**, 17004 (2002); I. J. Lee, D. S. Chow, W. G. Clark, M. J. Strouse, M. J. Naughton, P. M. Chaikin, and S. E. Brown, Phys. Rev. B **68**, 092510 (2003).
[41] R. W. Cherng and C. A. R. Sá de Melo, Phys. Rev. B **67**, 212505 (2002).
[42] C. M. Varma and A. Zawadowski, Phys. Rev. B **32**, 7399 (1985).
[43] J. C. Nickel, Thèse de troisième cycle, Université Paris 11, Paris, 2004.
[44] D. Zanchi, Europhys. Lett. **55**, 376 (2001).
[45] See, for instance, D. Poilblanc, M. Heritier, G. Montambaux, and P. Lederer, J. Phys. C **19**, L321 (1986).